Postharvest Biology and Technology 214 (2024) 112949

Contents lists available at ScienceDirect

Postharvest Biology and Technology

journal homepage: www.elsevier.com/locate/postharvbio

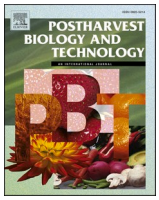

Optimizing ventilated packaging design for strawberries: Assessing the impact on fruit quality from farm to retailer using physics-based modeling

Elisabeth Tobler [a,b], Chandrima Shrivastava [a], Deniz Turan [b], Fátima Pereira da Silva [c], Celine Verreydt [a,b], Leo Lukasse [c], Thijs Defraeye [a,b,*]

[a] Empa, Swiss Federal Laboratories for Materials Science and Technology, Laboratory for Biomimetic Membranes and Textiles, Lerchenfeldstrasse 5, St. Gallen CH-9014, Switzerland
[b] Wageningen University and Research, Food Quality and Design, Department of Agrotechnology and Food Sciences, Bornse Weilanden 9, Wageningen 6708 WG, the Netherlands
[c] Wageningen Food & Biobased Research, P.O. Box 17, Bornse Weilanden 9, Wageningen 6700 AA, the Netherlands

ARTICLE INFO

Keywords:
Ventilated Packaging Design
Multiphysics modeling
Simulations
Supply Chain
Food loss
Quality preservation

ABSTRACT

Amongst fruits and vegetables, strawberries (*Fragaria* × *ananassa*) are one of the most perishable products. Consequently, it is challenging to maintain their quality until they reach the consumer. Therefore, keeping optimal hygrothermal conditions around the berries from farm to the consumer is crucial to preserving them and avoiding food loss. Using ventilated packaging design is an established way to address this technological, economic, and environmental problem. Until now, strawberry packaging is often designed using a trial-and-error approach, and a multitude of packaging designs exist. Ideally, the packaging should be designed in such a way that it provides the best preservation of the fruit all the way from farm to retailer. This is challenging since the hygrothermal conditions change significantly along the supply chain. In this study, we use physics-based modeling to evaluate new strawberry packaging designs in regard to cooling performance, risk of condensation, mass loss, and respiration-driven shelf life of the fruit and assess their performance along the whole post-harvest export supply chain from Spain to Switzerland. Twelve packaging designs for strawberries with existing and newly-designed vent hole configurations were investigated. Simulations quantified how the berries physiologically and hygrothermally evolve inside these packages along the whole post-harvest supply chain. Implementing appropriate ventilation in open-and top-sealed trays for strawberries can help to minimize losses along the post-harvest supply chain. As commonly known, strawberries cool significantly faster in better-ventilated trays than in unventilated trays, and condensation-based time of wetness could be reduced by 45% by adding additional ventilation holes in a top-sealed tray. The height of the secondary packaging, the total opening area (TOA), the size, and the placement of the vents have a substantial influence on the performance of the packaging. We recommend a TOA between 5.5% and 7% and a diameter of the vents between 5 and 12 mm. Also, they should be evenly distributed. However, there is always a trade-off in packaging design: a reduced risk of condensation comes along with a higher mass loss of the strawberries. Strawberry packaging models enabled a unique insight into the evolution of the fruits along the supply chain and visualized the spatial distribution of condensation and mass loss inside the package.

1. Introduction

Fresh fruits and vegetables are among the most wasted foods because they are highly perishable (Kelly et al., 2019). For strawberries (*Fragaria* × *ananassa*), the losses are estimated to be up to 40% from farm to consumer (Trinetta et al., 2020). Their high respiration rate is one of the basic causes of their high perishability (Castelló et al., 2010). Furthermore, they are susceptible to moisture loss and mechanical damage since they have a soft texture and no thick peel that protects them (Colussi

Abbreviations: ANOVA, analysis of variance; RANS, Reynolds-averaged Navier–Stokes; TOA,, Total opening area in the flow direction [%]; TOW, Time of wetness due to condensation [h].

* Corresponding author at: Empa, Swiss Federal Laboratories for Materials Science and Technology, Laboratory for Biomimetic Membranes and Textiles, Lerchenfeldstrasse 5, St. Gallen CH-9014, Switzerland.
E-mail address: thijs.defraeye@empa.ch (T. Defraeye).

https://doi.org/10.1016/j.postharvbio.2024.112949
Received 10 January 2024; Received in revised form 4 April 2024; Accepted 4 April 2024
Available online 11 May 2024

Nomenclature

Symbols

a_w	Water activity of strawberries [-]
A	Biochemical respiration-driven fruit quality [%]
c_l	Concentration of liquid water [mol m^{-3}]
$c_{p,a}$	Specific heat capacity of air [J $kg^{-1}K^{-1}$]
$c_{p,f}$	Specific heat capacity of strawberry fruit [J kg^{-1} K^{-1}]
c_{sat}	Saturation concentration of water vapor [mol m^{-3}]
c_v	Concentration of water vapor [mol m^{-3}]
C_μ	Turbulence model constant [-]
$D_{v,a}$	Diffusion coefficient of water vapor in air [m^2 s^{-1}]
$E_{a,quality}$	Activation energy of rate constant for kinetic quality model [J mol^{-1}]
f	Pre-exponential respiration coefficient [-]
g	Exponential respiration coefficient [-]
g_{evap}	Water evaporation flux [kg m^2 s^{-1}]
G	Source term for moisture transport [kg m^{-3} s^{-1}]
H	Source term for the time of wetness [h]
k_a	Thermal conductivity of air [W $m^{-1}K^{-1}$]
k_f	Thermal conductivity of strawberry fruit [W $m^{-1}K^{-1}$]
$k_{p,cardboard}$	Thermal conductivity of cardboard [W $m^{-1}K^{-1}$]
$k_{p,plastic}$	Thermal conductivity of plastic film [W $m^{-1}K^{-1}$]
$k_{0,quality}$	Reference kinetic rate constant for respiration-driven quality loss [s^{-1}]
$k_{quality}$	Kinetic rate constant for respiration-driven quality loss [s^{-1}]
k_{skin}	Strawberry skin resistance to moisture transport [m s^{-1}]
k_T	Turbulent kinetic energy [J kg^{-1}] or [m^2 s^{-2}]
K	Evaporation rate factor [m s^{-1}]
M_v	Molar mass of water vapor [kg mol^{-1}]
$\mathbf{n}$	Normal vector [-]
n	Order of reaction in the kinetic model
Q_{10}	Temperature coefficient for reaction rates [-]
Q_{resp}	Volumetric heat of respiration [W m^{-3}]
R	Universal gas constant [J mol^{-1} K^{-1}]
t	Time [s]
$t_{7/8}$	Seven-eighths cooling time [s]
T_a	Air temperature [K]
T_f	Fruit temperature [K]
$\mathbf{u}$	Velocity field vector
$x_{p,cardboard}$	Thickness of cardboard [mm]
$x_{p,plastic}$	Thickness of plastic film [mm]

Greek symbols

γ	Dimensionless temperature [-]
δ_a	Water vapor permeability of air [kg m^{-1} s^{-1} Pa^{-1}]
$\delta_{cardboard}$	Water vapor permeability of cardboard [kg m^{-1} s^{-1} Pa^{-1}]
$\delta_{plastic}$	Water vapor permeability of plastic film [kg m^{-1} s^{-1} Pa^{-1}]
ΔP	Pressure loss across the package [Pa]
∇	Vector differential operator [Pa s]
ε	Rate of dissipation of the turbulent kinetic energy [m^2 s^{-3}]
μ	Fluid viscosity [Pa s]
μ_p	Water vapor resistance factor [-]
μ_T	Turbulent component of viscosity [Pa s]
ξ	Pressure loss coefficient [Pa s^2 m^{-6}]
ρ_a	Density of air [kg m^{-3}]
ρ_f	Density of strawberry [kg m^{-3}]
ρ_p	Density of packaging material [kg m^{-3}]
ϕ_a	Relative humidity of air [%]

Subscripts

a	air
f	strawberry fruit
p	packaging
0	reference conditions
evap	evaporation
resp	respiration
in	in
l	liquid water
out	out
quality	quality
sat	saturated
skin	skin of the strawberry
T	turbulent
t	time
v	vapor

et al., 2021). These metabolic processes are temperature-driven, and consequently, cooling and proper handling of fresh horticultural products help to minimize losses in the post-harvest supply chain (Shoji et al., 2022). Also, strawberries are non-climacteric fruits, which means that they need to be harvested at nearly optimal maturity and ripeness. Moreover, temperature fluctuations at high relative humidity should be avoided to minimize condensation on the fruit surface because that favors the growth of molds (Ktenioudaki et al., 2019). Drivers of spoilage and the consequences of improper handling and condensation often stay unseen until the mold spores germinate and grow at the retail stage. Gray mold rot, induced by *Botrytis cinerea*, is the major cause of the immense post-harvest losses of strawberries (Schudel et al., 2022). To meet the high-quality marketability requirements for strawberries, maintaining optimal hygrothermal conditions around the products during the whole post-harvest supply chain is essential because it helps to slow down respiration and transpiration and therefore prolongs their shelf life (Mukama et al., 2020). Fortunately, the optimal hygrothermal conditions for most fruits and vegetables are known: strawberries should be ideally kept between 0 and 2 °C and 90–95% relative humidity (Ktenioudaki et al., 2019). It is the responsibility of transporters and retailers to keep the products within a narrow range of these conditions until they are made available to the consumers at the retail store. However, it is often the case that the temperature during the cold chain fluctuates and deviates from the optimal conditions. This temperature history information can be obtained by placing air temperature sensors in the cargo. Hence, it can be identified where temperature changes occur. In commercial supply chains of fruits and vegetables, the collection of temperature data, however, often occurs only during the transportation from the pack-house to the distribution center and no insight into the full supply chain is available. (Shoji et al., 2022). In order to preserve the ideal hygrothermal condition around the fruit, the use of appropriate ventilated packaging plays a key role.

The packaging design of horticultural products should consider multiple performance parameters to function efficiently along the whole supply chain, from pre-cooling to the retail store (Berry et al., 2017). Furthermore, packaging should protect the products from mechanical damage, physiological disorders, and diseases and allow efficient and uniform cooling of the products (Defraeye et al., 2015). Also, product parameters such as the initial microbial load play a role (Linke et al., 2021). Strawberry trays should ideally be designed with vent holes to facilitate airflow through the package. Vent area (in the direction of the flow), vent shape, number, and position are important elements that can contribute to uniform airflow and consequently affect the efficiency of the cooling (Pathare et al., 2012; Delele et al., 2013). The cooling rate depends primarily on the heat transfer between the cooling air and the product and is closely related to the airflow in the package (Zou et al.,

2006). Hence, better ventilated packaging cools the product faster. So far, studies on ventilated packaging have mainly focused on cooling performance during pre-cooling or transport but did not take the other unit operations of the supply chain into account. Several studies also focused on mechanical strength of boxes, the energy efficiency of the fan system, and condensation during the supply chain (Bovi et al., 2019). Delele et al., 2013 observed in their study about packaging design of oranges that there is only a minimal difference in the 7/8 cooling time by increasing the vent area from 7% to 9% or to 11%, respectively. Therefore, increasing the vent area to a certain value is not advantageous anymore but rather compromises the strength of the packaging. Similar results were obtained by De Castro et al., (2004): Increasing the vent area over 8% did not lead to better cooling. Wang et al., (2019) recommended in a more recent study a vent area of 8.5% of clamshells for optimal cooling of strawberries and uniformity when they are placed in a secondary package with a vent area of 9.4%.

Shrivastava et al., 2023 recently developed physics-based digital twins of 21 different commercially available ventilated packages of strawberries to mimic their post-harvest life from a farm in Spain to a retail store in Switzerland. With this technique, measured sensor data was translated into multiple actionable metrics, which help stakeholders make decisions, and it is possible to explain where and why losses occur. The above-mentioned study considered open trays, top-sealed trays, ventilated clamshells, and flow-wrapped packages. So far, the design of these existing packages was mainly based on a trial and error approach and did not ensure enough protection and preservation of the products inside (Cagnon et al., 2013). These packages could still be optimized more with respect to their ventilation pattern (size, location, form) to increase food preservation.

Evolved from the before mentioned research, the aim of this study was to design and evaluate new packages to improve food preservation. To achieve this goal, we translate the impact of packaging metrics, such as the height of the transport boxes (secondary packaging), the total opening area (TOA), and the placement of vents, into several final fruit quality attributes and on the cooling performance. Based on the analysis of the quality attributes, an optimized packaging design for strawberries was proposed. Physics-based models of 12 different strawberry trays were designed. A crucial input of these models was the temperature sensor data along the whole supply chain, as these models employ mechanic simulations to mimic how the quality of the fruit evolves in-silico along that simulated supply chain. Until now, physics-based modeling in combination with supply chain sensor data has not been used for optimizing packaging designs. However, there are various advantages: It allows to customize and simulate multiple packaging designs in a much shorter time period than with real experiments and gives unique insights into the hygrothermal conditions inside a tray. Also, minimal differences in their performance can be detected, and environmental conditions can be implemented and adjusted.

2. Materials and methods

2.1. The strawberry supply chain and its hygrothermal conditions

In this section, the strawberry supply chain is introduced in detail. Although every supply chain has its individual layout and hygrothermal conditions, the key unit operations the berries go through are the same for domestic or transnational chains (Fig. 1). This study simulates the hygrothermal conditions of a strawberry supply chain from Spain to a distribution center in Switzerland as reported by (Shoji et al., 2022; Shrivastava et al., 2023) as a use case, which is a distance of 2100 km.

Ideally, strawberries are harvested at the required maturity stage in the early morning when the outside air temperature is still rather cool to reduce the field heat stored in the fruit. Also, their surface should be dry to avoid fungal problems later in the chain. The berries are manually picked and directly sorted by the pickers on the fields. To minimize handling, they are often already packed into the final trays. They should be kept in the shadow on the field and be transported to a cooled pack house as soon as possible (within one hour). In this study, it is assumed that the temperature is 20 °C and the relative humidity is 55% on the field during harvest, based on previous studies (Shoji et al., 2022). In the packhouse, the first quality checks are done, the trays are labeled and palletized before they are cooled by forced-air cooling prior to transport. The overall appearance (color, size, shape, and damage) is controlled in each batch as well as the flavor and the sugar content. This is done by a sensory test and a Brix analysis. The individual trays are placed in carton transport boxes (secondary packaging) which are stacked and stabilized with straps and corner posts and precooled under forced air for up to 3 h at approximately 2 °C (D. Wang et al., 2019). This means that a fan forces cold air horizontally at a high velocity through the pallets (Mercier et al., 2019). Ideally, the berries are picked and transported on the same day. For transport, they should be loaded into a trailer, which is precooled as well, without stopping the cold chain to avoid rewarming. Temperature logging during transport is an essential part of quality control. In general, a single logger is placed on the top of the last pallet loaded on the passenger side of each trailer. Nevertheless, temperature varies inside a trailer and is, amongst others, dependent on the power of the fan, the loading pattern of the pallets, the airflow resistance of the packages, the initial fruit temperatures, and the weather. Furthermore, this logged temperature represents the air temperature and not the actual fruit temperature which also depends on the respiration and heat transfer processes of the fruit (Shoji et al., 2022). In Switzerland, normally, the refrigerated trailers arrive at the distribution center in the morning. However, the transport duration can vary a lot and take up to several days. In this study, we assume the duration of the transport to be 1.2 d. Immediately after arrival at the distribution center, the before-mentioned quality tests are performed again with a random selection of berries. If the quality assessment result is in alignment with the respective requirements, the pallets are sorted and organized for re-distribution to local retail stores, which is happening preferably within the same day. If not, the respective pallets are stored in cold rooms at 2 °C. From re-distribution onwards, the berries are transported and stored with other fruits and vegetables together. The temperature fluctuates around 10 °C during re-distribution. After arrival at the retailer, the berries are stored in cold rooms (10 °C) overnight at the retailer and displayed in uncooled shelves (20 °C) in the early morning. Furthermore, the relative humidity at retail stores is 45%, which is far below the optimum storage conditions for strawberries. Previous measurements showed that the relative humidity during transport and storage is quite constant at 80% (Shoji et al., 2022; Shrivastava et al., 2023).

A simplified hygrothermal profile of the post-harvest supply chain of strawberries from a farm in Spain to a retail store in Switzerland has been rebuilt based on sensor data, literature, previous studies, and discussions with stakeholders (Fig. 2). This temperature profile will be used as input in the simulations. The temperature profile of the refrigerated transport between Spain and the distribution center in Switzerland was

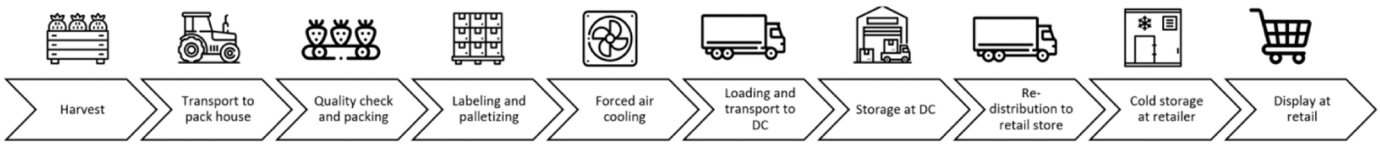

Fig. 1. Key unit operations of a typical import strawberry supply chain from Spain to Switzerland.

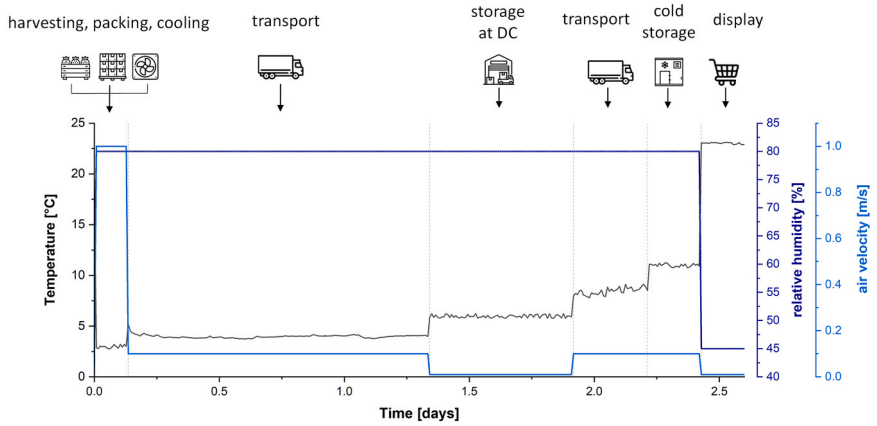

Fig. 2. Hygrothermal profile of the strawberry supply chain and air velocity mimicked in this study.

derived from the air temperature analysis of 68 actual berry road transports between November 2021 and April 2022 on this route. The data was retrieved from the sensors, which are generally put in every cargo. TempTale® RF (TTRF) temperature loggers, which have a resolution of 0.1 °C and an accuracy of 0.55 °C in the temperature range between −18 °C to 50 °C, were used. The temperature was logged every 11.5 min. One sensor was placed on the top of the last pallet loaded on the passenger side of each trailer. Time-temperature data could be accessed via the software ColdStream (Sensitech). Large temperature fluctuations can occur during transport. However, from the 68 analyzed berry transports, the average of the temperature along the trip and the average transport duration were considered as input for the digital twin models. The temperature profiles of the other operation units, as well as the values of the relative humidity and the airflow rates, were chosen based on previous studies and data from literature (Schudel et al., 2022; Shoji et al., 2022; Shrivastava et al., 2023). It was assumed that the berries stay about 13 h at the distribution center at 6 ± 1 °C before being redistributed to local retail stores. Temperatures were ramped up until the berries were displayed in the retail store shelves to minimize condensation. They stayed on the shelves for 4 h before this simulated supply chain ended. The relative humidity from after harvest until the retail store was set at 80% and at the retail store shelf at 45%. The mimicked supply chain had an overall length of 2.6 d. By subjecting all designed trays to identical conditions, we can effectively evaluate relative differences between the various packaging designs created.

2.2. Continuum multiphysics model

In this section, the computational domain, with its implemented physics and conditions, and the simulated variants of the packaging designs, are presented. An illustration of the geometrical model of a standard open tray filled with strawberries is shown in Fig. 3. The computational domain includes the berry tray with strawberries in it, which is surrounded by an air tunnel without bypass on the sides and below the package. Physical properties and parameters to quantify heat- and moisture transport in the computational domain are shown in Table 2, Section 2.2.7.

2.2.1. Computational domain and initial and boundary conditions

The models used in this study were based on the model of Shrivastava et al., 2023. Each modeled tray was filled with 16 strawberries in the same symmetric form, size, and weight. One berry weighed 16.3 g, had a surface area of 33.06×10^{-4} m^2 and a volume of 16.9×10^{-6} m^3. They were stacked in the same way in each tray. The 16 berries were intended to fill a tray of 250 g even if they weighed 260.8 g, which is a typically used commercial weight in which strawberries are sold. Sales-wise, a certain amount of mass loss along the supply chain is expected and therefore extra product is weighted to take this into account, as this is normally required by the retailer. The tray was placed in a virtual wind tunnel with a length of 90 cm and a width of 11.5 cm. The height of the tunnel was representative for the height of the secondary packaging box, in which typically 8–12 trays are placed in. In turn, this represents how close the trays are stacked on top of each other. Therefore, depending on the analysis that was conducted, this height was 8, 8.5, 9, or 10 cm. However, in industry the packages are packed rather dense, and therefore, the height is kept minimal. To mimic the hygrothermal conditions along the supply chain, airflow was modeled horizontally from one side of the tunnel, namely the inlet. The open-top carton boxes (secondary packaging), in which the trays are stacked, have few or no vent holes on the bottom of the package. As a result,

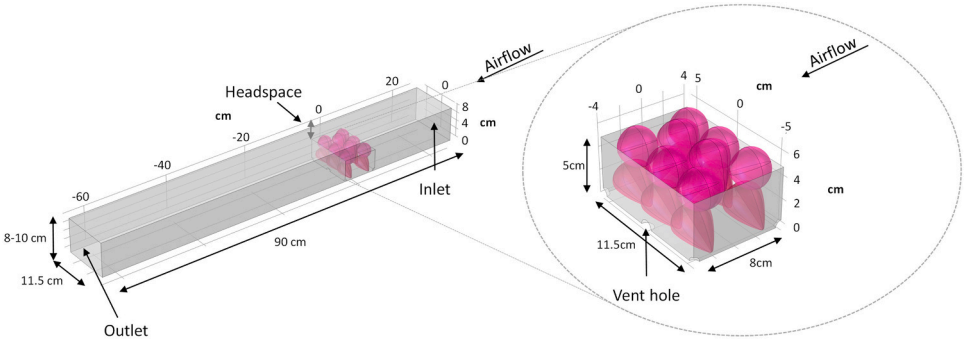

Fig. 3. Schematic overview of the computational domain of a standard open tray. It includes the berry tray, in which strawberries are directly placed. The tray was placed in a virtual wind tunnel without bypass on the sides and below the package. To mimic the hygrothermal conditions along the supply chain, airflow was modeled horizontally from one side of the tunnel, namely the inlet. The height of the tunnel is representative for the height of the secondary packaging.

airflow is mainly horizontal in the package as this is the only possible airflow direction. To avoid influences of the boundaries on the airflow and heat transfer, the outlet was modeled far enough away on the downstream section. The initial temperature and relative humidity of the simulated air were set to 20 °C and 55%, respectively, which corresponds to the conditions at harvest. Also, the initial temperature of the berries was set to 20 °C.

2.2.2. Simulated variants of packaging design

In this study, 6 new models of ventilated cardboard open trays and 6 new models of ventilated cardboard trays with a polypropylene sealing layer on top were created (Table 1). Additionally, one tray for each packaging type without additional vent holes on the side (basic trays) was created, which represent the packages that can currently be found in industry. These trays just have the characteristic vents on the bottom in the middle, and in the corners. The total opening area (TOA) in flow direction, as well as the placement and the number of vents, was varying between the trays. The analyzed total opening areas ranged from 1.1% to 7.2%, distributed between 3 and 19 single vents per side of a tray. Two trays each have the same TOA but a different number, size, and placement of the vents to assess the impact of these parameters. The top-sealed trays were modeled with 5 additional vent holes in the sealing layer, as this is common for such packages. Because flow is only simulated horizontally, this might not have a big impact on the cooling process, but it can influence the condensation inside the packaging along the supply chain. Note that the top-sealed trays are 2 cm higher than the open trays. If the berries were not packed, the cooling air would not be disrupted by the packaging walls, and therefore, more air would directly hit the berries. This seems to be the ideal case to cool berries as fast as possible. Accordingly, this case was mimicked as well. Table 1 shows the configuration of all packaging designs that were evaluated in this study.

2.2.3. Air flow

The airflow velocity at the inlet of the tunnel was set based on the respective operation unit. 0.01 m s^{-1} for refrigerated storage and retail, 0.1 m s^{-1} for refrigerated transport, and 1.0 m s^{-1} for pre-cooling (Schudel, et al., 2022; Shrivastava et al., 2023). Air was assumed to be incompressible. To model the nonisothermal flow, the Boussinesq approximation was used. Therefore, it was assumed that variations in air density do not affect the airflow field. Thus, the continuity equation of the Navier-Stokes equation can be reduced to the form presented in Eq. 1, where $\mathbf{u}$ is the air velocity field vector [m s^{-1}].

$$\nabla \cdot \mathbf{u} = 0 \tag{1}$$

The momentum equation of the Navier-Stokes equations is presented in Eq. 2, where ρ_α is the density of air [kg m^{-3}], P is the atmospheric pressure [Pa], and $\mu + \mu_T$ represents the effective viscosity [Pa s]. The subscript T stands for turbulent. F is the momentum source term and is equal to zero since buoyant forces were neglected. The transient term, which would indicate changes in velocity over time, was also neglected because a steady state airflow field was modeled for each operation unit. Hence, temperature and moisture did not influence the flow field.

$$\rho_\alpha(\mathbf{u} \bullet \nabla \mathbf{u}) = -\nabla P + \nabla \bullet [(\mu + \mu_T)(\nabla \mathbf{u} + (\nabla \mathbf{u})^T] + F \tag{2}$$

A k-$\boldsymbol{\varepsilon}$ turbulence model with wall functions was implemented to model turbulent flow in the computational domain. The turbulent part of the viscosity μ_T [Pa s] was computed as expressed in Eq. 3, where $C\mu$ is the constant of the turbulence model, k_T the turbulent kinetic energy, and ε the dissipation of the turbulent kinetic energy. The airflow at the inlet was modeled with a turbulence intensity of 0.05%.

$$\mu_T = \frac{\rho_a C_\mu k_T^2}{\varepsilon} \tag{3}$$

2.2.4. Heat transfer

2.2.4.1. Heat transfer in air. The equation of the heat transfer in the air domain is presented in Eq. 4. It describes air temperature changes over time due to convection and conduction. $c_{p,a}$ represents the specific heat capacity of air [J kg^{-1} K^{-1}], T_a is the temperature of the air [K], k_a is the thermal conductivity of the air [W m^{-1} K^{-1}], and t is the time [s].

$$\rho_a c_{p,a} \frac{\partial T_a}{\partial t} + \rho_a c_{p,a}(\mathbf{u} \bullet \nabla T_a) + \nabla \bullet (-k_a \nabla T_a) = 0 \tag{4}$$

2.2.4.2. Heat transfer in the berries. The heat transfer in the berry domain is described in Eq. 5, where T_f is the fruit temperature [K] at any time t, k_f is the thermal conductivity of the strawberries [W m^{-1} K^{-1}], $c_{p,f}$ the specific heat capacity of the berries [J kg^{-1} K-1] and ρ_f their density [kg m^{-3}]. Q_{resp} [W m^{-3}], which indicates the heat generated by the berries, was estimated by their CO_2 production rate as function of temperature. It was assumed that for every mg CO_2 produced, 10.7 joules of heat is generated. The according equation is presented in Eq. 6. The coefficients f (3.668 $\times 10^{-4}$) and g (3.0330) are strawberry specific respiration coefficients (Becker et al., 1996). Also, it was assumed that the physical properties of the berries remain constant during the process. Therefore, shriveling due to mass loss was neglected. Hence, the respiratory heat of strawberries at 0 °C is approximately 40 mW kg^{-1} and 394 mW kg^{-1} at 20 °C.

$$\rho_f c_{p,f} \frac{\partial T_f}{\partial t} + \nabla \bullet (-k_f \nabla T_f) = Q_{resp} \tag{5}$$

$$Q_{resp} = \frac{10.7f}{2300}\left(\frac{9T_f}{5} + 32\right)^g \rho_f \tag{6}$$

2.2.4.3. Heat transfer across the packaging. The packaging boundaries were modeled as thin layers with thermal resistance. The thermal resistance of the packages is, however low, and the heat capacity is assumed to be negligible. It was assumed that the heat flux across the package is proportional to the temperature difference between the in- and outside of the packaging. The equation of this thermally thin approximation is presented in Eq. 7.

$$-\mathbf{n}_{in} \bullet (-k_p \nabla T_{a,in}) = \frac{k_p}{x_p}(T_{a,out} - T_{a,in}) = \mathbf{n}_{out} \bullet (-k_p \nabla T_{a,out}) \tag{7}$$

The terms $-\mathbf{n}_{in} \bullet (-k_p \nabla T_{a,in})$ and $\mathbf{n}_{out} \bullet (-k_p \nabla T_{a,out})$ describe the heat flux into and out of the packaging, where k[W m^{-1} K^{-1}] is the thermal conductivity of the cardboard, and the plastic layer, of which the trays were made of, and x_p [m] is their thickness. T_a [°C] is the air temperature at the in- and outside of the packaging and $\mathbf{n}$ a normal vector.

2.2.5. Moisture transport

Water is present in a liquid phase, inside the berries or as condensed water on the surfaces of the berries, and in a gas phase, as water vapor in the air. Condensation and evaporation play crucial roles and these processes are highly temperature dependent. The moisture transport in the different domains of the model is described in the following section.

2.2.5.1. Moisture transport in air. The equation for moisture transport in the air is presented in Eq. 8.

$$M_v \frac{\partial c_v}{\partial_t} + M_v \mathbf{u} \bullet \nabla c_v + \nabla \bullet (-M_v D_{v,a} \nabla c_v) = G \tag{8}$$

M_v is the molar mass of the water vapor [kg mol^{-1}], c_v is the concentration of the water vapor [mol m^{-3}], and $D_{v,a}$ the water vapor diffusion coefficient in the air [m^2 s^{-1}]. G [kg m^{-3} s^{-1}] is the moisture source term and accounts for the addition or removal of moisture into the air (Becker et al., 1996; ASHRAE, 2010; Concha-Meyer et al., 2018). At the surface of the fruit, there is a moisture flux into the air due to

Table 1
Overview of all open and top-sealed trays analyzed in this study. The basic open-and top-sealed basic trays are frequently seen in Switzerland. The open-and top-sealed trays 1–6 are new created designs.

Package name	Isometric view	Isometric view, transparent	Bottom view	Side view	Materials	TOA in flow direction [%]
Open trays						
Open basic tray					Paperboard	1.7
Open tray 1					Paperboard	3.4
Open tray 2					Paperboard	3.4
Open tray 3					Paperboard	5.6
Open tray 4					Paperboard	5.6
Open tray 5					Paperboard	7.2
Open tray 6					Paperboard	7.3
Top-sealed trays						
Top-sealed basic tray					Paperboard, polypropylene	1.1
Top-sealed 1					Paperboard, polypropylene	3.5
Top-sealed 2					Paperboard, polypropylene	3.5
Top-sealed 3					Paperboard, polypropylene	5.7
Top-sealed 4					Paperboard, polypropylene	5.7
Top-sealed 5					Paperboard, polypropylene	7.2
Top-sealed 6					Paperboard, polypropylene	7.1
No packaging						
No packaging					-	100

transpiration of the berries and due to evaporation of the condensate on the surface of the berries. The background of the term G is further explained in the following. The connection between the water vapor concentration and the saturated water vapor concentration c_{sat} [mol m^{-3}] derives from the relative humidity ϕ_a and is presented in Eq. 9.

$$c_v = \phi_a c_{sat} \tag{9}$$

2.2.5.2. Moisture transport across the packaging walls. The packaging walls were modeled as vapor barriers to model discontinuous moisture content across the packaging walls. Therefore, the moisture transfer coefficient β [kg m^{-2} s^{-1}] that accounts for vapor diffusion, was used. The resistance is typically very large, so it will likely not influence the moisture transport, which is mainly convective. β was defined as presented in Eq. 10. This factor is the ratio of the water vapor permeability of air to the water vapor permeability of the material.

$$\beta = \frac{\delta p_{sat}}{\mu x_p} \tag{10}$$

δ is the vapor permeability of the packaging material [kg m^{-1} s^{-1} Pa^{-1}], p_{sat} is the saturation pressure of water vapor [Pa], μ the water vapor resistance factor (dimensionless), and x_p [m] the thickness of the packaging material. The temperature dependency of the material was neglected.

2.2.5.3. Moisture transport at the strawberry surface due to transpiration and condensation. During post-harvest storage and handling, strawberries lose moisture through their skin via transpiration. Also condensation can take place when the temperature of the fruit or the tray is below the dew point temperature of the air. The water flux at the fruit surface g_{evap} [kg m^2 s^{-1}] due to transpiration was computed using Eq. 11.

$$\mathbf{n} \bullet g_{evap} = k_{skin} M_v (a_w c_{sat} - c_v) \tag{11}$$

In the equation above, **n** is the normal vector at the fruit's surface pointing into the air domain, k_{skin} is the skin transfer coefficient accounting for skin resistance to moisture transport and also the resistance of the boundary layer to moisture transport, which is however, often, very low [m s^{-1}], a_w is the water activity on the surface of the berry [-], which was assumed to be 1, and c_{sat} the saturation concentration of water vapor which is assumed to be present below the skin surface [mol m^{-3}]. If $c_{sat} > c_v$, the fruit transpires and release water into the air. However, if $c_{sat} < c_v$, condensation occurs. Therefore, the same equation was used to calculate the water vapor condensation on the berry.

2.2.6. Kinetic quality model

After harvest, strawberries undergo visible and physiological decay, senescence, as a consequence of their respiration process, which is significantly influenced by temperature. This overall quality decay, which was here modeled as overall fruit quality index A [%], is a result of biochemical and enzymatic reactions within the fruit (Nunes, 2009). To predict the evolution of this temperature-driven overall quality of strawberries, a first-order kinetic rate law model was implemented. The kinetic rate law represents an exponential decay in fruit quality as function of time as shown in Eq. 12, where $k_{quality}$ is the temperature-dependent rate constant [s^{-1}], n is the order of the reaction, which is 1 here, and T_f is the volume average berry temperature [K] (Corradini, 2018).

$$-\frac{\mathrm{A(t)}}{\mathrm{dt}} = k_{quality}(T_f)\mathrm{A}^n \tag{12}$$

It was assumed that the supply chain started immediately after the berries were harvested, such that the initial fruit quality index A was equal to 100%. The respiration-driven fruit quality index for strawberries at different constant storage temperatures was used to calibrate the model (Shrivastava et al., 2023). Based on previous studies and literature (Jalali et al., 2020; Shrivastava, Schudel, et al., 2022) a threshold of 20% was used as a minimum quality threshold. If the quality drops below 20%, the fruits are assumed to be not marketable anymore. This threshold can be chosen arbitrarily to some extent as the model parameters are calibrated based on the shelf life. The choice of another threshold will still induce the same shelf life when stored at optimal temperature.

A Q_{10} value of 2.75 was considered for the berries (Tano et al., 2009; Shrivastava et al., 2023). The Q_{10} value is a measure that expresses the temperature dependency of reactions (Tano et al., 2009). In this case, it means that a temperature increase or decrease of 10 °C, increases or decreases, respectively, the reaction speed with a factor of 2.75 (Eq. 13). Also, the rate constant is not constant over time but temperature dependent ($k_{quality}$ (T_f)). This temperature dependency is incorporated into the model through the Arrhenius equation, which is presented in Eq. 14. Here, $k_{0,quality}$ is a constant [s^{-1}], $E_{a,quality}$ is the activation energy [J mol^{-1}], R the universal gas constant [J mol^{-1} K^{-1}].

$$Q_{10} = \frac{k_{quality}(\mathrm{T}+10)}{k_{quality}(T)} \tag{13}$$

$$k_{quality}(T_f) = k_{0,quality} \quad e^{\frac{-E_{a,quality}}{RT_f}} \tag{14}$$

2.2.7. Material properties

Table 2

Table 2
Physical properties and parameters to quantify heat- and moisture transport in the computational domain.

Parameter	Symbol	Value	Unit	Reference
Specific heat capacity of air	$c_{p,a}$	1006	J kg^{-1} K^{-1}	(ASHRAE, 2010)
Thermal conductivity air	k_a	0.024	W m^{-1} K^{-1}	(ASHRAE, 2010)
Vapor permeability of air (at 23 °C)	δ_{air}	1.95 $\times 10^{-10}$	Kg m^{-1} s^{-1} Pa^{-1}	(ASHRAE, 2010)
Thermal conductivity strawberry	k_f	0.6	W m^{-1} K^{-1}	(Becker et al., 1996; Shrivastava et al., 2023)
Density of strawberry	ρ_f	961	Kg m^{-3}	(Concha-Meyer et al., 2018; Shrivastava et al., 2023)
Specific heat capacity of the strawberry	$c_{p,f}$	4000	J kg^{-1} K^{-1}	(Becker et al., 1996; Shrivastava et al., 2023)
Skin moisture transfer coefficient	k_{skin}	1.77 $\times 10^{-3}$	m s^{-1}	(Becker et al., 1996; Shrivastava et al., 2023)
Quality rate constant	$k_{0,quality}$	3.55$\times 10^{6}$	s^{-1}	(Shrivastava et al., 2023)
Thermal conductivity of cardboard	$k_{p,cardboard}$	0.066	W m^{-1} K^{-1}	(Shrivastava et al., 2023)
Thermal conductivity of plastic layer	$k_{p,plastic}$	0.036	W m^{-1} K^{-1}	(Ngo et al., 2016; Shrivastava et al., 2023)
Thickness of cardboard	$x_{p,cardboard}$	0.51	mm	(Shrivastava et al., 2023)
Thickness of plastic	$x_{p,plastic}$	0.03	mm	(Shrivastava et al., 2023)
Vapor permeability of cardboard (at 25 °C)	$\delta_{cardboard}$	4.3 $\times 10^{-13}$	Kg m^{-1} s^{-1} Pa^{-1}	(Shrivastava et al., 2023)
Vapor permeability of plastic layer (at 25 °C)	$\delta_{plastic}$	2.3 $\times 10^{-17}$	Kg m^{-1} s^{-1} Pa^{-1}	(Bastarrachea et al., 2011; Shrivastava et al., 2023; J. Wang et al., 2018)
Vapor resistance factor of cardboard	$\mu_{cardboard}$	450	-	(Shrivastava et al., 2023)
Vapor resistance factor of plastic film	$\mu_{plastic}$	8.5 $\times 10^{6}$	-	(Shrivastava et al., 2023)

2.3. Quality related actionable metrics

The data obtained from the digital twin models was further processed into selected actionable metrics, which are suitable for the strawberry supply chain and can be used by stakeholders to make decisions. These are quantifying the quality, are easy to handle, and help to compare the different packages. For each of the 16 strawberries in a tray, a probe of the average pulp temperature and the mass flux across the surface was created. These probes are virtual and can be applied to analyze and monitor the behavior of physical quantities within specific domains of a model. Therefore, each berry could be monitored independently from the others and heterogeneity within one tray and between different trays could be studied.

2.3.1. Seven-eighths cooling time

Seven-eighths cooling time (7/8 cooling time or $t_{7/8}$), the time which is required to reduce the temperature difference between the berries and the cooling air by seven-eighths, is a useful parameter to assess the cooling performance of fruits and vegetables. Rapid cooling of fruits and vegetables has been shown to extend their shelf life (Elansari and Mostafa, 2020; Liberty et al., 2013; Wu et al., 2019). It can be evaluated based on the dimensionless cooling curve Y, which is presented in Eq. 15. In this equation, T_p is the average fruit temperature, $T_{p,0}$ is the initial temperature of the product and T_a is the set cooling air temperature.

$$Y = \frac{T_p(t) - T_a}{T_{p,0} - T_a} \tag{15}$$

Consequently, the 7/8 cooling time refers to the time when Y drops below 0.125. The simulations of the cooling process were done independently of the simulations in which hygrothermal data along the whole supply chain was implemented. The temperature of the cooling air was kept constant at 4 °C and the relative humidity at 80%. The airspeed was set to 1 m s^{-1} as it is usually the case during pre-cooling. The initial temperature of the berries was set to 20 °C.

2.3.2. Mass loss

The cumulative mass loss over the entire supply chain [%] was calculated numerically with the equation presented in Eq. 16, wherefore the moisture loss due to transpiration was considered. In the equation, $\int g_{evap}$ [kg m^{-2}] refers to the integrated evaporation flux over time at each point on the surface of the berries. The assumed surface area of one berry was 0.003306 m^2 and the assumed surface area of one berry was 0.01628 kg (Shrivastava et al., 2023). Hence, it indicates the mass loss [%] at every point on the surface of each berry, and therefore, this is a suitable way to present the variability as well.

$$Mass\ loss\ [\%] = \frac{\int g_{evap} \times 0.003306 m^2 \times 100}{0.01628 kg} \tag{16}$$

2.3.3. Time of wetness due to condensation

In our study, the risk of condensation was evaluated as the time of wetness (TOW [h]). It refers to the integrated time at which condensation takes place or the relative humidity at the surface of the berry is higher than 97%. The TOW should be as low as possible since it is related to the risk of mold growth (Linke and Geyer, 2013). TOW was expressed in hours and calculated by the model at every point of the surface of the berries separately. It was calculated by an ordinary differential equation shown in Eq. 17, where H [h] represents the source term.

$$\frac{d\left(\frac{TOW}{3600}\right)}{dt} = H \qquad H = \left\{ \begin{array}{l} 1, g_{evap} < 0 or \varnothing_a > 97 \\ 0, else \end{array} \right\} \tag{17}$$

2.3.4. Remaining shelf life

On the basis of the quality model described in 2.2.6, the remaining shelf life was predicted. The remaining shelf life [d] was calculated with the equation presented in Eq. 18, assuming a storage temperature on the shelf of 20 °C.

$$Shelf\ life\ (t) = \frac{-\ln\left(\frac{A(t)}{20}\right)}{k_{quality(20°C)}} \times (24 \times 3600) \tag{18}$$

2.4. Packaging performance metrics

2.4.1. Total open area in the direction of the flow

The total opening area in the direction of the flow (TOA [%]) indicates the open surface area of the package in flow direction. In other words, the surface area of the vent holes. The influence of the TOA on the cooling performance has already been investigated in many studies (Berry et al., 2017; Shrivastava et al., 2023).

2.4.2. Pressure loss across the package

The lower the resistance to airflow, the more air is inclined to flow through the package and not around of the package and also, less energy is needed to cool down the berries. The static pressure loss across the package ΔP [Pa] was assessed at the inlet of the channel and at the open boundary at the end of the channel. This was done by placing virtual probes on these boundaries to measure the pressure difference. The pressure loss is a function of the superficial airspeed, which is defined as the volumetric flow rate divided by the cross-sectional area at the inlet. Therefore, local changes of the airspeed due to the berry packaging were neglected. A parametric study with inlet airspeeds of 0.01, 0.05, 0.1, 0.2, 0.5, 1.0 and 1.5 m s^{-1} was performed. Accordingly, a pressure loss coefficient (ξ, Pa s^2 m^{-6}) was calculated with Eq. 19, which shows a quadratic relation with the volumetric flow rate. $A_{channel}$ is the cross-sectional area of the channel [m^2], U_{inlet} [m s^{-1}] is the superficial airspeed at the inlet.

$$\Delta P = \xi (A_{channel} U_{inlet})^2 \tag{19}$$

2.5. Numerical implementation and simulation

The model was based on the model of Shrivastava et al., 2023. The physics-based digital twin models were developed in COMSOL Multiphysics (version 6.0), a finite element simulation software. For the airflow, the Turbulent Flow k-Ɛ interface was used, and for the heat- and moisture transport models, Heat Transfer in Moist Air and Moisture Transport in Air were used. These models were combined by the Multiphysics Couplings feature. The kinetic quality model and the model for computing transpiration were implemented by the Ordinary Differential Equation interface. The computational mesh consisted of 0.5 $\times 10^6$ - 1.3 $\times 10^6$ tetrahedral elements depending on the configuration. The mesh settings were defined based on a grid sensitivity analysis (Shrivastava et al., 2023).

The airflow study was calculated in two steps: first, the wall distance initialization, and second, the stationary flow field. The flow field was assumed to be independent of temperature and moisture and was computed for the different airspeeds occurring along the supply chain (0.01, 0.1, and 1.0 m s-1) with a parametric sweep. The airflow was calculated in advance and used as input for the transient simulations along the simulated supply chain. For the wall distance initialization, a fully-coupled generalized minimal residual method (GMRES) solver was used, and for the stationary flow field, a segregated solver scheme, namely the MUltifrontal Massively Parallel sparse direct Solver (MUMPS) was employed. The relative solver tolerance was set to 0.001.

In the second part of the study, heat and moisture transports and the quality models were computed over time in a transient simulation. Each unit operation of the supply chain was implemented as a step, which is linked to the according input parameters. Therefore, a segregated solver scheme with a tolerance of 10^{-4} was implemented. Also, the MUMPS solver scheme was used for heat transport, and a PARAllel DIrect sparse SOlver (PARADISO) scheme was used for moisture transport. The interval of the input data was set to 11.5 min, which corresponds to the

interval of the sensors. A free time-stepping algorithm was implemented, in which the time step was determined by the solver tolerance.

2.6. Data processing and statistical analysis

Simulation data was further processed and analyzed with Microsoft Excel (Office 365, Version 2016). For each conducted simulation experiment, statistical analysis of the simulated output parameters among different packages was carried out by using the graphing and analyzing software Origin 2022 (Version 9.9.0.225). An ANOVA (analysis of variance) was performed where the Tukey test was used to compare mean values of respective physical quantities in each strawberry, and Levene's test to test the homogeneity of variance. Results are expressed as mean ± standard deviation, and the significance level was set to $p < 0.05$.

2.7. Validity of the model

In the study of Shrivastava et al. (2023), a validation study where temperature and humidity values, predicted by the model, were compared with values measured in climate chamber experiments, was per-formed. Overall, a very good agreement between the predicted and measured temperature was observed. Additionally, the averaged value of the simulated relative humidity across the entire supply chain was within 2% of the measured value. Similarly, the study of Schudel et al., (2022), combined experiments and mechanistic modeling to compare selected ventilated packaging types for strawberries from farm to retailer. The models employed in their study were based on those developed by Shrivastava et al. (2023) as well. Hence, an extensive evaluation of such model's performance and respective experiments has already been made.

3. Results and discussion

3.1. Impact of the height of the transport boxes on strawberries' cooling performance and quality metrics

We aim to investigate the impact of a particular parameter of the computational study, namely the height of the transport box (secondary packaging). In industry, the secondary packaging – the carton boxes in which the trays are placed – varies, especially in height. In the computational domain, we therefore adjusted the height of the tunnel representing the height transport box. To analyze its impact, the seven-eighths cooling time (SECT [h]), the time of wetness due to condensation (TOW [h]), and the mass loss of berries in open- and top-sealed basic trays and selected ventilated trays were assessed for different tunnel heights. The heights were 8, 8.5, 9, and 10 cm. The selected ventilated trays had the designs of open-and top-sealed tray 6 (2.2.2 Simulated variants of packaging design).

3.1.1. Impact on the seven-eighths cooling time

Fig. 4 shows the impact of the tunnel height on the seven-eighths cooling time in open-and top-sealed basic- and ventilated trays. A higher height above the packaging leads to slower cooling. In trays with a high TOA, which are indicated as open ventilated trays and top-sealed ventilated trays, the impact is smaller than in the basic cases for open trays and top-sealed trays where the TOA is much smaller. Consequently, sufficient airflow that passes through the packaging, so a low height of the secondary packaging, contributes a lot to the reduction of the SECT and, moreover, reduces sensitivity to the height of the transport box. Smaller differences between the height of the trays and the secondary packaging lead not only to a shorter SECT in all tested trays but also reduces the heterogeneity within the trays. The shortest SECT was found in the top-sealed ventilated tray in a 8 cm tunnel. However, there was no significant difference in the SECT between all ventilated trays. The longest SECT was found in the top-sealed basic tray in a 10 cm tunnel, which is significantly longer than in all the other testes trays except the top-sealed basic tray in a 9 cm tunnel.

3.1.2. Impact on the time of wetness

Fig. 5 shows the impact of the tunnel height on the time of wetness due to condensation (TOW, [h]) after the 2.6 d simulated supply chain scenario. The TOW follows the same trend as the SECT: Ventilation contributes to a reduction of the TOW. The TOW is significantly higher in both basic tray scenarios simulated with a 10 cm tunnel compared to the same scenario simulated with an 8 cm tunnel. The observed differences within the ventilated trays are not significant. Hence, the influence of the height of the secondary packaging is smaller in ventilated trays and also smaller in open trays compared to top-sealed trays.

3.1.3. Impact on the mass loss

Fig. 6 shows the impact of the tunnel height on the mass loss after the 2.6 d simulated supply chain scenario. Interestingly, the trend of the mass loss is exactly the opposite of the trend of the SECT and the TOW. Hence, there is a trade-off between these quality metrics. A higher secondary packaging leads to a reduced mass loss of the berries along the supply chain. Berries in top-sealed basic trays lose the least mass, while berries in ventilated top-sealed trays lose the most mass, comparatively.

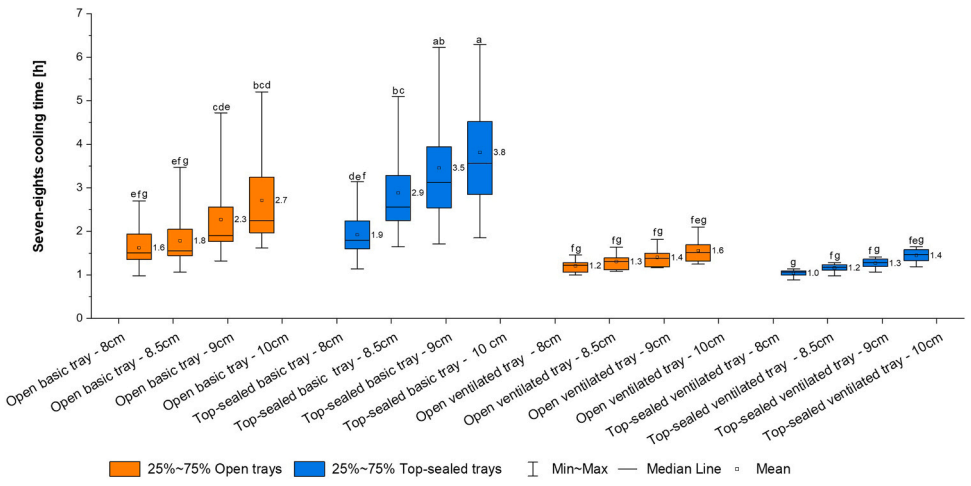

Fig. 4. Impact of the tunnel height on the seven-eighths cooling time (SECT) of berries packed in open- and top-sealed basic- and ventilated trays. The ventilated trays had a TOA of 7.1–7.2%. Each boxplot represents one tray with 16 strawberries. The numbers next to the box correspond to the mean value of the SECT. Values with the same letter are not significantly different, $p<0.05$.

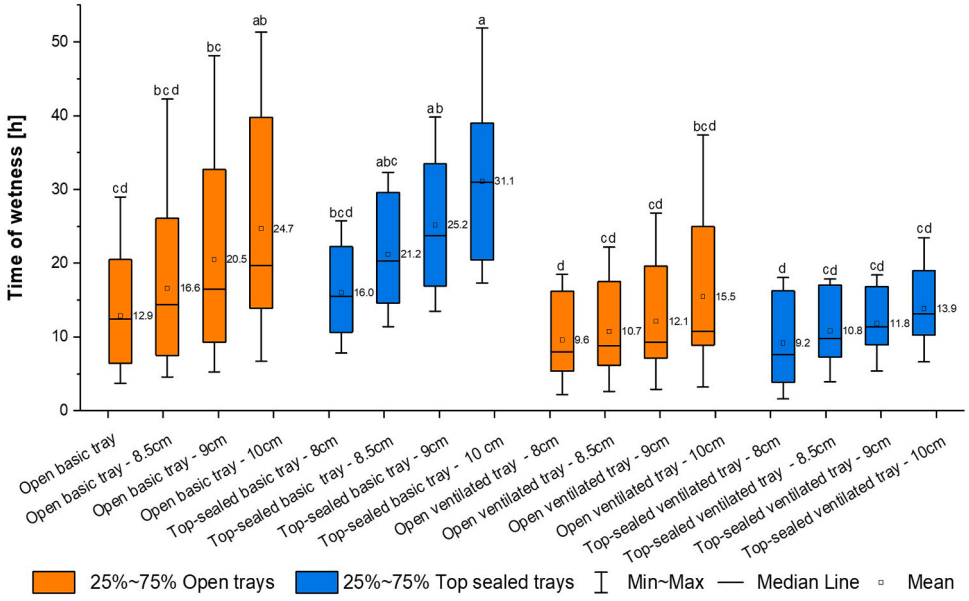

Fig. 5. Impact of the tunnel height on the time of wetness due to condensation (TOW, [h]) after the 2.6 d simulated supply chain scenario. The ventilated trays had a TOA of 7.1–7.2%. Each boxplot represents one tray with 16 strawberries. The numbers next to the box correspond to the mean value of the TOW. Values with the same letter are not significantly different, $p<0.05$.

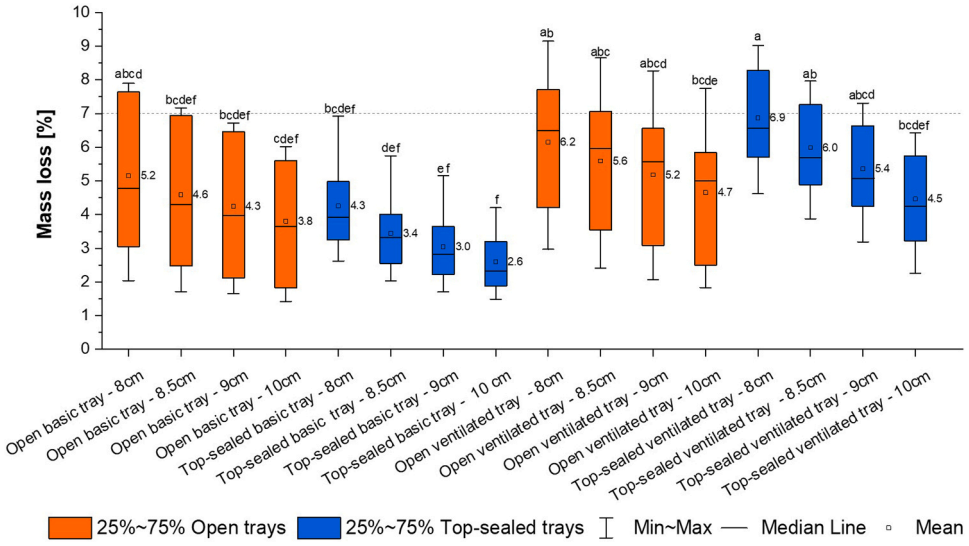

Fig. 6. Impact of the tunnel height on the mass loss after the 2.6 d simulated supply chain scenario. The ventilated trays had a TOA of 7.1–7.2%. The mass loss [%] of the strawberries in the different trays were evaluated after the 2.6 d simulated supply chain. Each boxplot represent the average mass loss per berry in the respective tray. The numbers next to the box show the mean value of the tray. Values with the same letter are not significantly different, $p<0.05$. The dotted line indicates the threshold of 7%.

There is a significant difference in mass loss of berries in ventilated top-sealed trays with a tunnel height of 8 cm compared to 10 cm. Within the other identical trays (open basic, open ventilated, top-sealed basic), there are no significant differences. Moreover, in open trays, more variability within one tray can be observed. In this study, we set a threshold of 7% mass loss on average. Above this level, it was assumed that consumers would reject the product (Shrivastava et al., 2023).

The smaller the tunnel height, which represents the height of the secondary packaging, the more air is pushed through the vents, and less is bypassing over the top. Therefore, this specific height and the presence of vent holes have a substantial influence on the airflow inside the package and, consequently, on the quality of the berries. Ventilation reduces sensitivity to the height of the secondary packaging. Therefore, we would recommend using secondary packaging with a height of the two short sides just 2–3 cm higher than the height of the primary tray, while the height of the long sides is minimal, to ensure proper cooling. Note, however, higher secondary packaging will induce a larger pressure resistance. Air gaps between pallets are essential because the air needs to flow through the pallets in a trailer. Also, air around the pallets experiences less resistance when cargo is not packed too tight. In summary, a small height above the primary packaging, so low secondary packaging is beneficial for cooling. However, this assumes that all air is pushed through the pallets of fruit, which happens for example in a precooler. In a trailer, airflow bypass can occur around the pallets, by which the net airflow going through a pallet will be less for low secondary packaging, as the airflow resistance will be higher.

The condensation-based TOW is related to the risk of mold growth and should consequently be as low as possible. The TOW follows the

same trend as the SECT since ventilation also contributes to a reduction of the TOW. The higher the tunnel height, the less air flows through the package, and accordingly, more condensation can be observed along the whole supply chain (Fig. 5). Also, the influence is bigger in the two base case scenarios compared to the properly ventilated scenarios. Hence, the influence of the secondary packaging is smaller in ventilated trays and also smaller in open trays compared to top-sealed trays since the air bypass inside the package is generally higher when the tray is open. However, well-ventilated packaging can remove warm air faster and, therefore, prevent condensation partly. Unfortunately, the trend of mass loss follows the opposite direction. More mass loss, which is a disadvantage, can be observed when the tunnel height is smaller. The reason for this trade-off will be discussed in chapter 3.3.

It is important to consider that the structure and adjustments on the computational domain have a significant influence on the output of such models. Here, it influences quality metrics as well. However, in this case, the simulations act as a valuable tool to identify relative differences between the individual packaging designs.

3.2. To what extent do packaging parameters influence cooling and the evolution of different quality parameters from farm to retail?

3.2.1. Airflow and aerodynamic performance

We aim to investigate the aerodynamic performance of the designed trays in this study. This was done by analyzing the pressure loss across the trays, so inlet minus outlet pressure, as a function of the volumetric flow rate. Also, this defines how much pressure the fans should deliver to push cool air through the package at a certain flow rate. Furthermore, we take a look into the airflow pattern inside different ventilated and non-ventilated trays. The simulations for the analyses in the following chapters were made with a channel height of 8 cm. This value was chosen based on the study above and because this gap size can be found in the industry.

Fig. 7 shows the airflow velocity profile during pre-cooling (inlet velocity of 1 m s^{-1}) from a side view perspective of the two basic open- and top-sealed trays, the open- and top-sealed ventilated tray 6, and of the no packaging. In all scenarios, the airflow gets accelerated above the package or the berries, respectively, because the airflow inside the packaging is limited, especially in the not ventilated trays, and there, the air experiences the most resistance to pass. However, vent holes in the direction of the flow allow airflow between the berries inside the packaging. The highest velocities inside the packaging can be observed in the top-sealed ventilated tray. Air jets with higher velocities than at the inlet arise due to the vents and the packaging. However, the airflow velocity profile is most homogenous in the no packaging scenario.

Fig. 8 shows the pressure loss as a function of the volumetric airflow rate across all designed open- and top-sealed trays with different vent hole arrangements and a different TOA and the no packaging scenario. The pressure was measured at the inlet and at the outlet of the air tunnel, and the corresponding pressure loss coefficients were determined. It can be seen that packaging evidently causes resistance to airflow, but it depends on the package- and vent design. The resistance induced by the berries is comparatively small. Clearly, lower airflow resistances were observed in open trays (orange colors) than in top-sealed trays (blue colors). Comparing the open trays and top-sealed trays individually, the pressure drop coefficients generally decrease with an increase in the TOA. The airflow resistance of all open trays is similar, whereas, in top-sealed trays, the TOA and the placement of the vents have a notable impact on the pressure loss. Top-sealed tray 6 has the same TOA as top-sealed tray 5. However, top-sealed tray 6 shows a noticeably lower resistance to airflow than top-sealed tray 5. Likewise, top-sealed tray 4 has a remarkably lower resistance to airflow than top-sealed tray 3, despite of the similar TOA. Hence, more but smaller vent holes can have a positive impact on the aerodynamic performance if the TOA is more than 5.5%.

The airflow pattern inside the trays and the pressure loss across the trays strongly depend on the presence of vent holes, including their size and placement on the side of the packaging walls. Vent holes in the direction of the flow allow airflow between the berries inside the packaging. Air jets with high velocities arise due to the vents, which improve the cooling of the berries. However, this is dependent on various parameters, such as the stacking of the fruit or the size of the vents. Ideally, the berries shall not block the vents, as it is simulated in the cases described in this study. In reality, this cannot be controlled.

The pressure drop is much lower in all open trays because air can flow over the package. Various studies have already observed this (De Castro et al., 2004; Getahun et al., 2017; Lufu et al., 2020). Also, Delele et al., 2013 reported that for a constant vent area, the pressure drop decreased with a larger number of vents. This was also observed in this study.

In packages with low resistance and thus a low pressure drop coefficient, less mechanical energy is needed to push the air through the package. Vent hole placement, TOA, package size, headspace inside the package, alignment of the secondary package, fruit stacking, and palletizing play an important role in commercial industry and should be considered together when choosing the packaging.

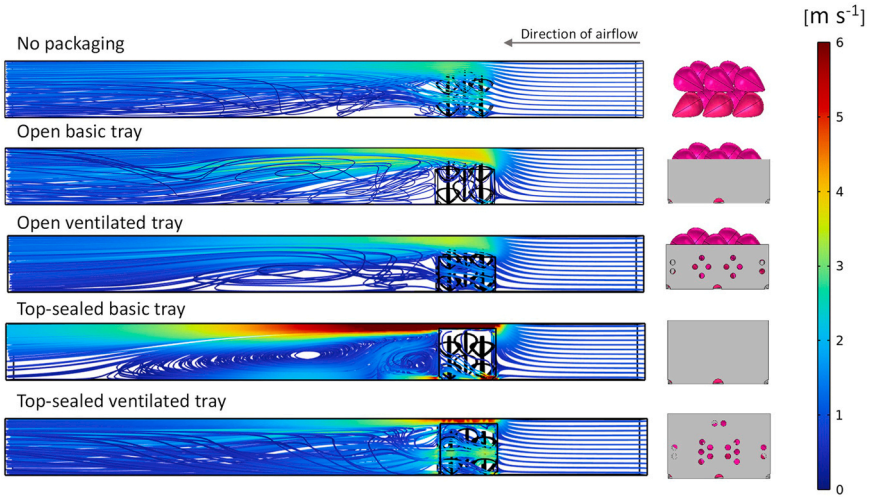

Fig. 7. Side view of the airflow velocity profile during pre-cooling of the two basic open- and top-sealed trays, the open-and top-sealed ventilated tray 6, and the no packaging scenario.

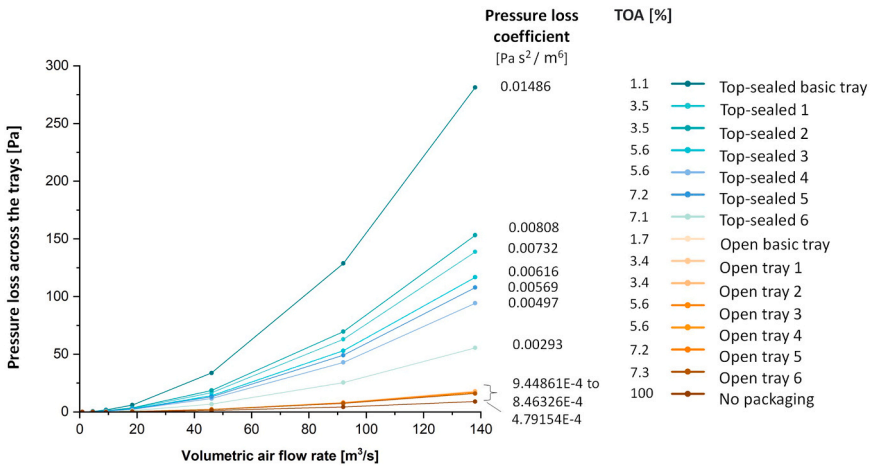

Fig. 8. Pressure loss across the trays as a function of the volumetric airflow rate through the computational domain. The pressure was measured at the inlet and the outlet of the air tunnel. The pressure loss coefficients were calculated by fitting a quadratic model in Microsoft Excel. The blue colored lines belong to the top-sealed trays, and the orange colored lines to the open trays.

3.2.2. *Cooling performance*

Fig. 9 shows the SECT of the berries in all designed open- and top-sealed trays. Each boxplot presents the mean value and the distribution of the temperatures of the 16 berries per tray. All but one ventilated package, the open tray 2, cooled down the berries significantly faster than the basic trays, which do not have additional vents on the side. This applies to both open- and top-sealed trays. However, differences are smaller in the open tray packages compared to top-sealed packages. Berries in the open basic tray need 1.62 ± 0.45 h to cool down to seven-eighth of the temperature difference between the initial fruit temperature and the cooling air, whereas the open trays 5 and 6, which showed to cool the fastest within the tested open trays, need 1.21 ± 0.17 h and 1.21 ± 0.15 h, respectively. Interestingly, the berries do not cool significantly faster without packaging compared to the berries in the ventilated open trays. Nevertheless, they cool more homogeneously. They need 0.94 ± 0.09 h to cool down to seven-eighths of the total temperature difference. The SECT of top-sealed trays 5 and 6, which had the highest TOA of all top-sealed trays, were 1.01 ± 0.11 h and 1.04 ± 0.07 h. Nonetheless, the berries inside these trays do not cool down significantly faster than the berries in the other ventilated top-sealed trays.

Berries in open trays are generally more exposed to the cooling air. Therefore, the differences between the basic tray and the ventilated trays are smaller. However, additional vent holes on the side of open trays can reduce the SECT by 25.3%. The SECT of berries in top-sealed trays could be reduced by 47.4% by placing vent holes. These additional vents increased the TOA from 1.1% to 7.2%. The SECT of all open- and top-sealed trays 3–6 have negligible differences. In a real-world setting, these differences would offset since the stacking of the berries or the placement in the cooling room and on the pallet have an additional impact. Hence, it can be concluded that not more than a TOA of 5.6% is needed to reduce the SECT and, therefore, cool the berries effectively. From TOAs > 5.6%, the arrangement of the vents is less important regarding the SECT. Already a TOA of 3.5%, as Open trays 1 and 2 and Top-sealed trays 1 and 2 reduce the SECT significantly. This can be seen as well in Fig. 10a. The airflow velocity is an important

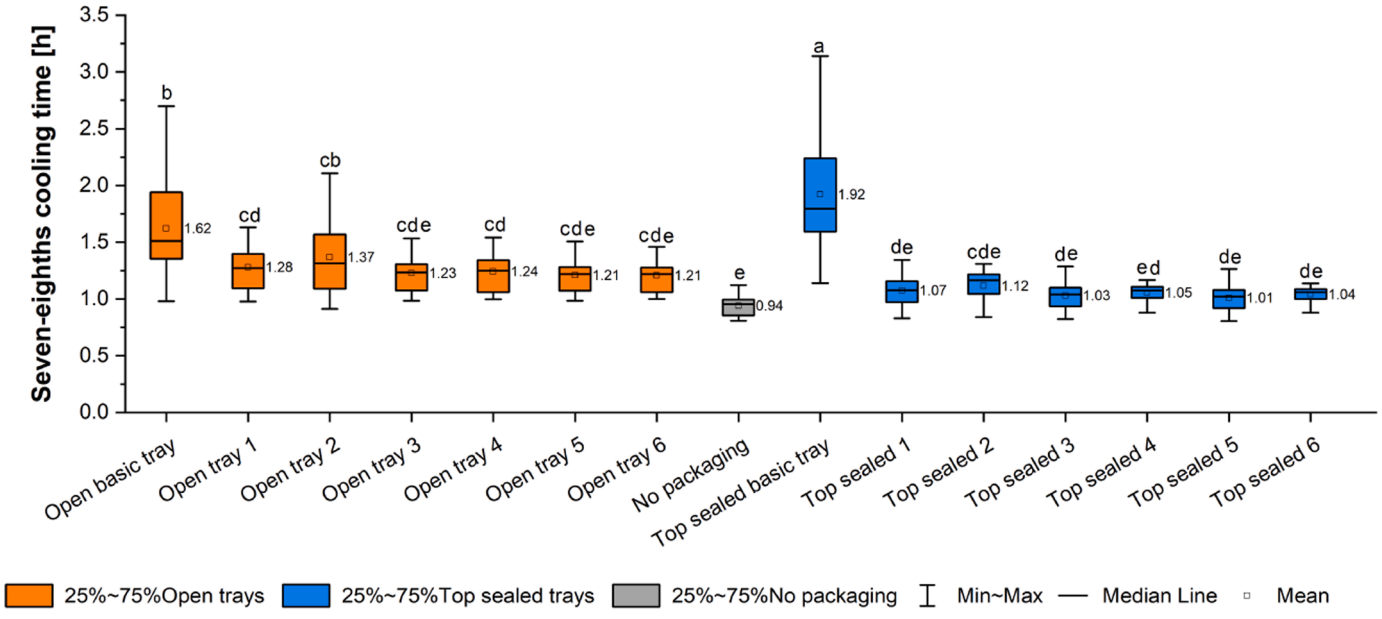

Fig. 9. Seven-eighths cooling time [h] of strawberries in different trays. Each boxplot represents one tray with 16 berries in it. The numbers next to the box show the mean value. Values with the same letter are not significantly different, $p<0.05$.

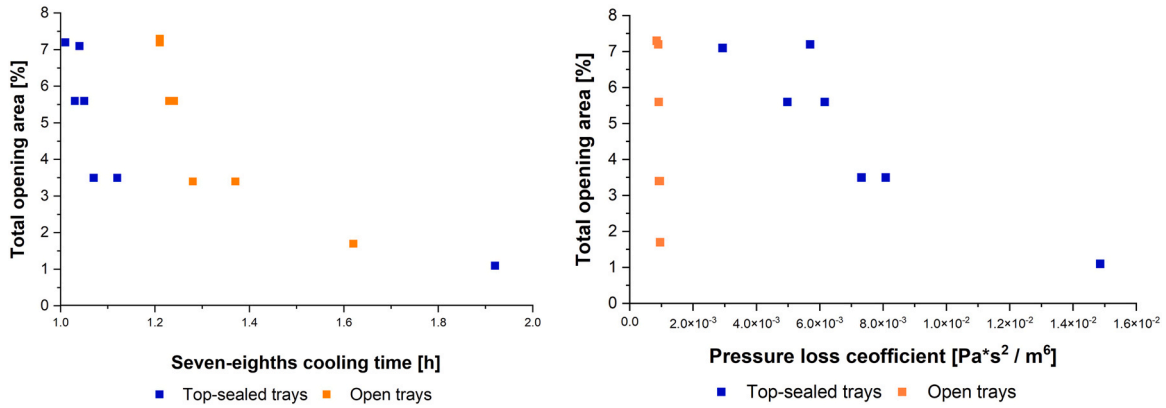

Fig. 10. (a) Seven-eighths cooling time and (b) pressure loss coefficient [Pa s^2 / m^6] as a function of the total opening area [%]. Each data point represents one package. Open trays are colored orange, and top-sealed trays are colored blue.

factor regarding cooling. The higher the airflow velocity, the faster the cooling (Defraeye et al., 2014). Since the air cannot flow through the packaging walls, it needs to escape through the vent holes or bypass over the top of the package. In top-sealed trays, more air flows through the vents with higher airspeeds than in open trays because they have less space above where it can pass too. Consequently, berries in top-sealed trays cool faster.

3.2.3. *Seven-eighths cooling time and pressure drop vs. uniformity and the total opening area of the vents*

As observed in the sections above, besides the TOA, the arrangement of the vents can influence the SECT and the pressure drop across the package. In open trays, however, the pressure drop is comparatively low in any case compared to top-sealed trays. Fig. 10 shows the SECT (a) as well pressure drop coefficient (b) as a function of the TOA.

A higher number of vents and a different arrangement of them – with the same TOA – leads to a lower pressure drop coefficient in top-sealed trays. The influence is bigger, the higher the TOA is. Because open trays have a large opening in general above the fruit, no remarkable differences can be observed. There is a weak correlation between TOA with the aerodynamic resistance of the package and the SECT, as this correlation is strongly dependent on the packaging type. Also, this implies that TOA is not necessarily a good design parameter to estimate the pressure resistance and the SECT.

It is important that the vent holes of the trays align with the vent holes in the secondary package to make sure that air can flow through. Furthermore, the secondary packaging - carton boxes which usually carry 8–10 trays – and the alignment of the pallets in cooling chambers, trailers, or containers will also influence the cooling performance, the pressure drop and the energy consumption. Additionally, it is unique for every shipment since berries are filled without a pattern in the trays, and also, there are always tiny gaps between packages. Nevertheless, open trays will perform more energy efficiently than top-sealed trays because a lot of air can pass over the tray.

3.2.4. *How do the selected quality metrics of strawberries evolve along the supply chain?*

For the consumers, the quality at the retail store, so at the end of the supply chain, is of interest. However, to sell the berries at their best possible quality, we need to know where in the supply chain losses occur. Therefore, Fig. 11 shows the evolution of the quality metrics of strawberries along the supply chain in an open basic tray and a top-sealed basic tray. The steeper the curve, the higher the rate of quality loss. The green curves show, that the respiration-driven remaining shelf life evolves similar in the open and top-sealed basic trays. Also, in both trays, the highest rates of condensation are found at the distribution center and at the retailer. However, the rates are higher for the top-sealed tray. At these stages in the supply chain, the airflow rates are low, and the temperature is higher than at the previous stage. During refrigerated transport, the risk of condensation is comparatively low. As observed before, this is, in turn, the unit operation where most mass loss occurs. Also, during display at the retailer, the rate of moisture loss is high. Hence, we conclude that high airspeeds are a major reason for mass loss besides high temperatures. The curve of the respiration-driven remaining shelf life confirms that high temperature is the main driver of respiration. Note that the curves would look different for top-sealed ventilated trays.

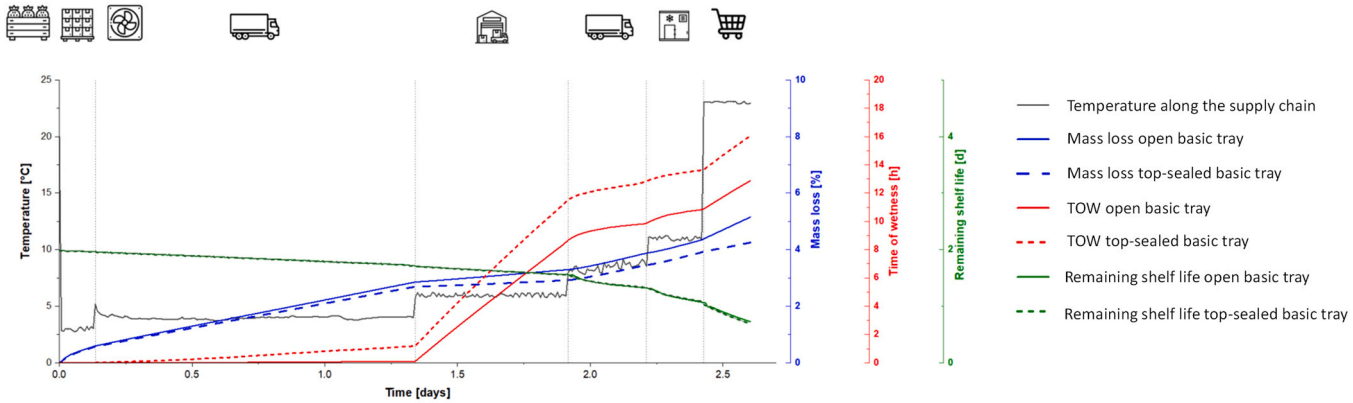

Fig. 11. Evolution of the quality metrics of strawberries along the supply chain in an open basic tray and a top-sealed basic tray.

3.2.5. Time of wetness due to condensation

We aim to identify in which tray the berries are most prone to condensation and in which regions of the packaging condensation occurs along the whole supply chain.

Fig. 12 shows the TOW of the strawberries in all the designed open- and top-sealed tray after the 2.6 d simulated supply chain (a) as well as the spatial distribution of the TOW inside well-ventilated trays and basic trays (b). There is no significant difference between the berries in the different open trays. However, the TOW could be reduced by 3.3 h as a result of the added vent holes. The spots at the downstream side, on the bottom, and the areas between the berries are most prone to condensation. In the top-sealed trays 5 and 6, with a TOA of 7.2%, the TOW could significantly be reduced compared to the top-sealed basic case. The obtained values were 8.83 ± 06.16 h and 9.19 ± 6.04 h, respectively, which is close to 7 h less than the TOW of the berries in the basic top-sealed tray. Even if there was no packaging around the berries, so if berries were hypothetically placed free in the airflow, condensation would take place in these areas due to the hygrothermal changes occurring in the supply chain. The simulated TOW for that case was 8.14 ± 5.25 h.

Condensation occurs in spots where cooling air cannot continuously remove the humid air inside the package and, therefore, where relative humidity becomes too high. The airflow is not only blocked by the packaging but also by the berries. Hence, condensation would occur as well without packaging, for example when berries are exposed to warm humid air. Overall, the formation of the air jets due to the vents has a beneficial impact on the TOW. As seen before, the air velocity becomes higher in top-sealed trays than in open trays. Hence, the time of wetness is highly dependent on the airflow rate and, therefore, on the ventilation capacity of the packaging.

Condensation depends on temperature fluctuations and happens when the berry surface is colder than the dew point temperature or when the air is saturated and cannot hold any more water. The dew point temperature is the temperature where condensation takes place. The air heats up faster than the berries in warm surroundings, and consequently, condensation on the surface of the berries happens. Therefore, it is important to keep the temperature not only low but also constant during refrigerated transport. Because the temperature at the retail store is around 20 °C and the relative humidity around 45%, it is beneficial to slowly ramp up the air temperature so that the temperature differences

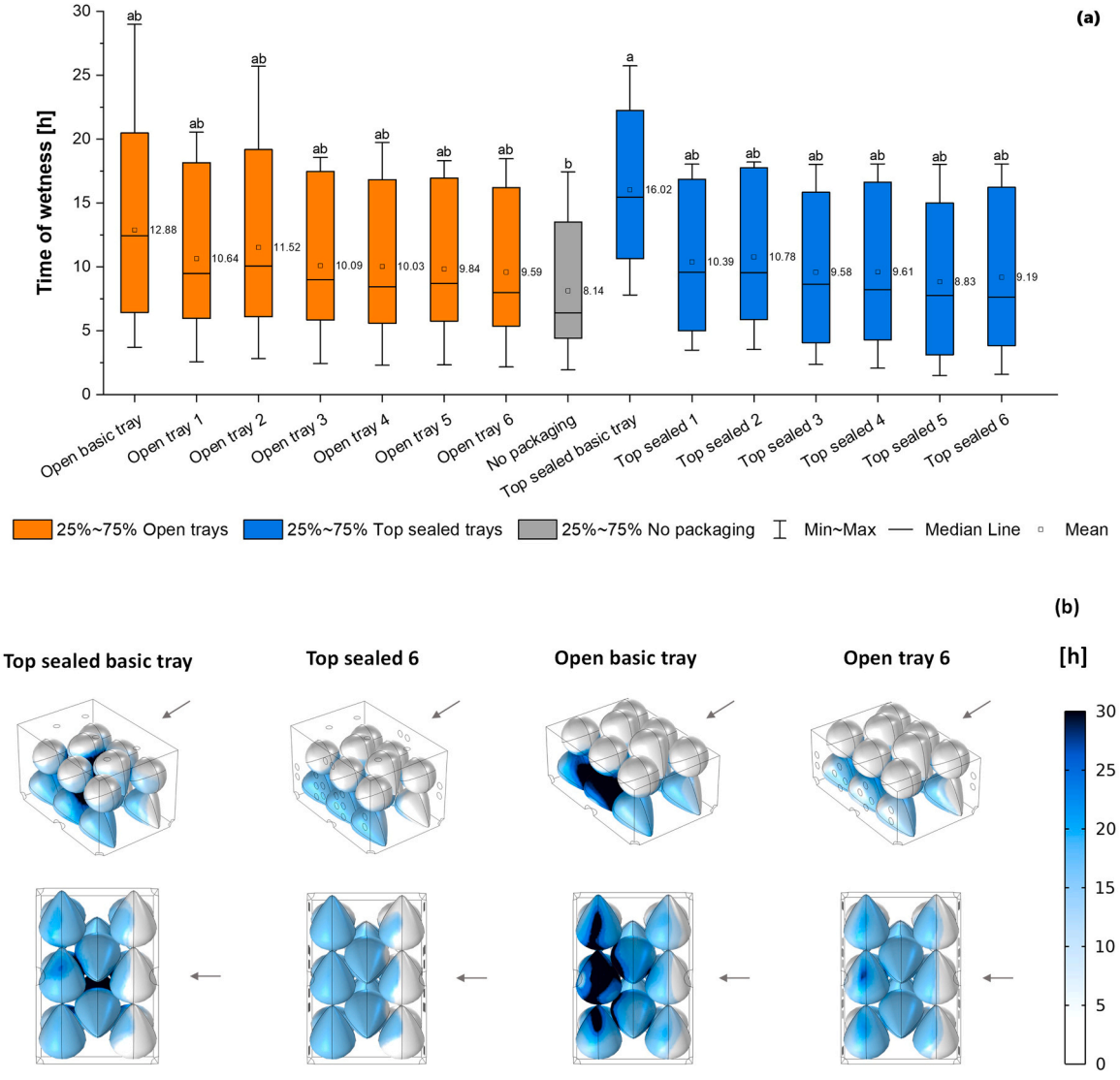

Fig. 12. Time of wetness [h] of strawberries in different trays after the 2.6 d simulated supply chain. (a) Each boxplot represents one tray with 16 berries in it. The numbers next to the box show the mean value. Values with the same letter are not significantly different, $p<0.05$. (b) Spatial variability of TOW in selected packages. The arrows indicate the direction of the airflow.

between the warm air and the cold berries are not too high. This is also a reason why the temperatures during refrigerated storage and re-distribution are not that low anymore in the supply chain that was monitored. However, a better approach to preserve the quality of the berries and minimize the risk of mold growth would be to keep the same cold temperature along the whole supply chain and display them in refrigerators at retail stores. Another option is to let the berries warm up prior to storage in retail stores in an environment that is at sufficiently low relative humidity to avoid condensation.

3.2.6. *Mass loss due to transpiration*

The expression mass loss is used interchangeably as moisture loss or weight loss, and the phenomenon is influenced by various pre- and post-harvest factors and occurs due to transpiration of the fruit (Lufu et al., 2020; Sousa-Gallagher et al., 2013). We aim to investigate how much mass the berries lost along their post-harvest journey. Preferably, as little as possible because the fruits and vegetables start to shrivel from a mass loss of 5–10% and are, therefore, not marketable anymore. Since fruits are sold by weight, mass loss also represents economic losses (Lufu et al., 2020; Robinson et al., 1975).

Fig. 13 shows the mass loss of the strawberries in all the designed open- and top-sealed trays after the 2.6 d simulated supply chain (a) as well as the spatial distribution of the mass loss inside selected trays (b). The least mass loss, which was 4.26 ± 1.29%, was observed in the basic top-sealed tray, and the highest mass loss, which was 7.11 ± 1.39%, was observed in top-sealed tray 5. There is no significant difference in mass loss of the berries in the different ventilated open- and top-sealed trays. However, a larger variability within the trays, but also within one single berry, was observed in the open trays compared to the top-sealed trays. Most berries in ventilated top-sealed trays lose up to 2.85% more moisture along the supply chain than in unventilated top-sealed trays, which is a significant difference. Only the berries in top-sealed tray 5 and without packaging exceed the threshold of 7%.

Besides the duration from farm to retail, other key drivers of mass loss along the supply chain are high temperatures, low relative humidity, and high airspeeds, which are, in turn, dependent on the packaging design. Therefore, the highest moisture loss rates are expected directly after harvest and also during pre-cooling as well as during display when the temperatures are rising and the relative humidity drops. Hence, berries in open tray packages are more susceptible to moisture loss at display than berries in top-sealed trays, but this depends on the ventilation openings of the latter. Generally, the ventilated trays are more susceptible to mass loss than the non-ventilated trays since air flows at a higher velocity through these trays. At higher airspeeds, moisture that possibly is on the surface of the berries can be transported away better. However, this leads to increased transpiration (Poós & Varju, 2020; Shrivastava et al., 2023). Berries on top of the open trays and close to a vent hole facing the direction of the flow were more affected than the berries in the middle. Although ventilated packaging design contributes to making cooling more efficient, it also leads to higher mass loss rates along the supply chain.

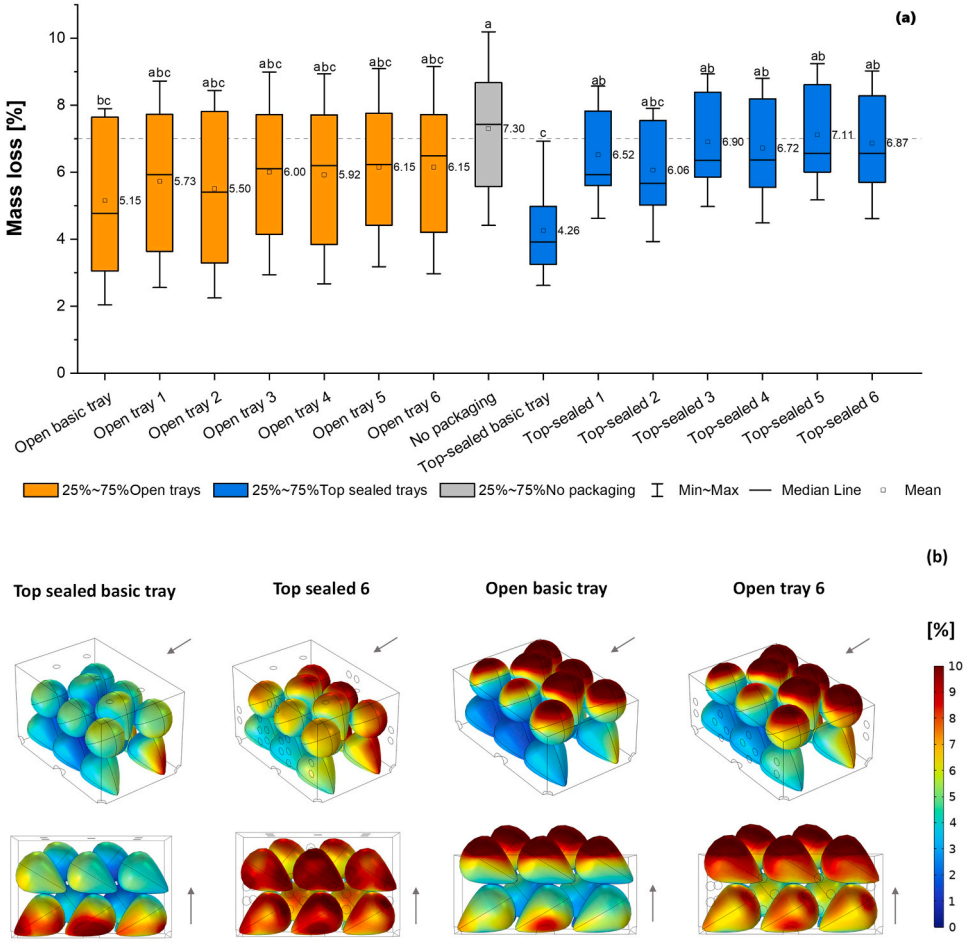

Fig. 13. Mass loss [%] of strawberries in different trays after the 2.6 d simulated supply chain. (a) Each boxplot represent the average mass loss per berry in the respective tray. The numbers next to the box show the mean value of the mass loss per tray. Values with the same letter are not significantly different, $p<0.05$. The dotted line indicates the threshold of 7%. (b) Spatial variability of the mass loss in selected packages. The arrows indicate the direction of the airflow.

3.2.7. Respiration-driven remaining shelf life

Fig. 14 shows the remaining respiration-driven shelf life of the strawberries in all the analyzed trays and of the no packaging scenario after the 2.6 d simulated supply chain. The strawberries in all open trays have a significantly longer remaining shelf life than all the berries in the ventilated top-sealed trays. Variations within the trays are bigger in all open trays and the biggest in the no-packaging scenario. However, the remaining shelf life of the berries in top-sealed trays is generally shorter. On average, berries can still be stored for 0.91 d (22 h) at 20 °C in open trays until the average consumer would reject them. In top-sealed trays, berries can be stored between 0.67 (16 h) and 0.81 d (19.5 h) at 20 °C on average until most of the consumer would reject them.

Berries have a small Biot number and, therefore, cool rather uniformly and adapt relatively fast to their surrounding temperature. Berries that cool down fast in a certain package also rewarm fast. However, because respiration is much higher in a hot environment, it is important to keep the berries cool. Directly after harvest – before pre-cooling – and during display at the retail store, the berries respire the most since temperatures are highest. Hence, proper pre-cooling is essential to preserve strawberries along the supply chain. If the berries were stored at 10 °C instead of 20 °C at the retail store, the respiration-driven shelf life would be extended to almost two days and up to 2.5 d at 5 °C. We can conclude that the packaging design has an impact on the thermal decay of strawberries along the supply chain and afterward in the retail phase. However, condensation and mass loss need to be considered as well in defining an overall shelf life.

3.3. What are the trade-offs in choosing the optimal packaging?

3.3.1. Condensation vs. mass loss vs. quality decay

Fig. 15 shows the trade-off between condensation and mass loss in all analyzed trays and the no-packaging scenario. Additionally, the data points are colored regarding their respiration-driven remaining shelf life. The results showed that the lower the TOW, the higher the mass loss. This is probably the most important quality-related trade-off in the packaging design of fresh fruits. It should be noted that the impact of the secondary packaging, as seen in chapter 3.1, has a major influence. Hence, with higher transport boxes, the relationship would be steeper:

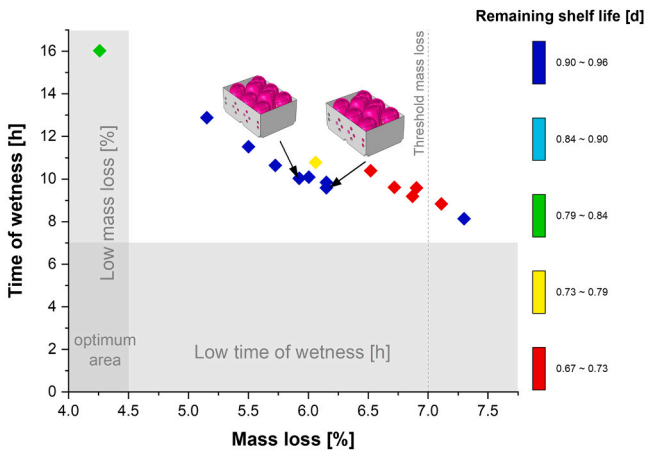

Fig. 15. Time of wetness [h] as a function of the mass loss [%]. Each dot represents one package. The values correspond to the values measured after the 2.6 d simulated supply chain. The data points are colored regarding their respiration-driven remaining shelf life. The vertical dotted line represents the threshold of mass loss where above most consumers would reject the product. The grey areas indicate the areas of low mass loss and low time of wetness, respectively. The optimum area would be, where the TOW and the mass loss are low. The data points of the suggested best-performing packages are indicated with an arrow and belong to Open tray 4 and 6.

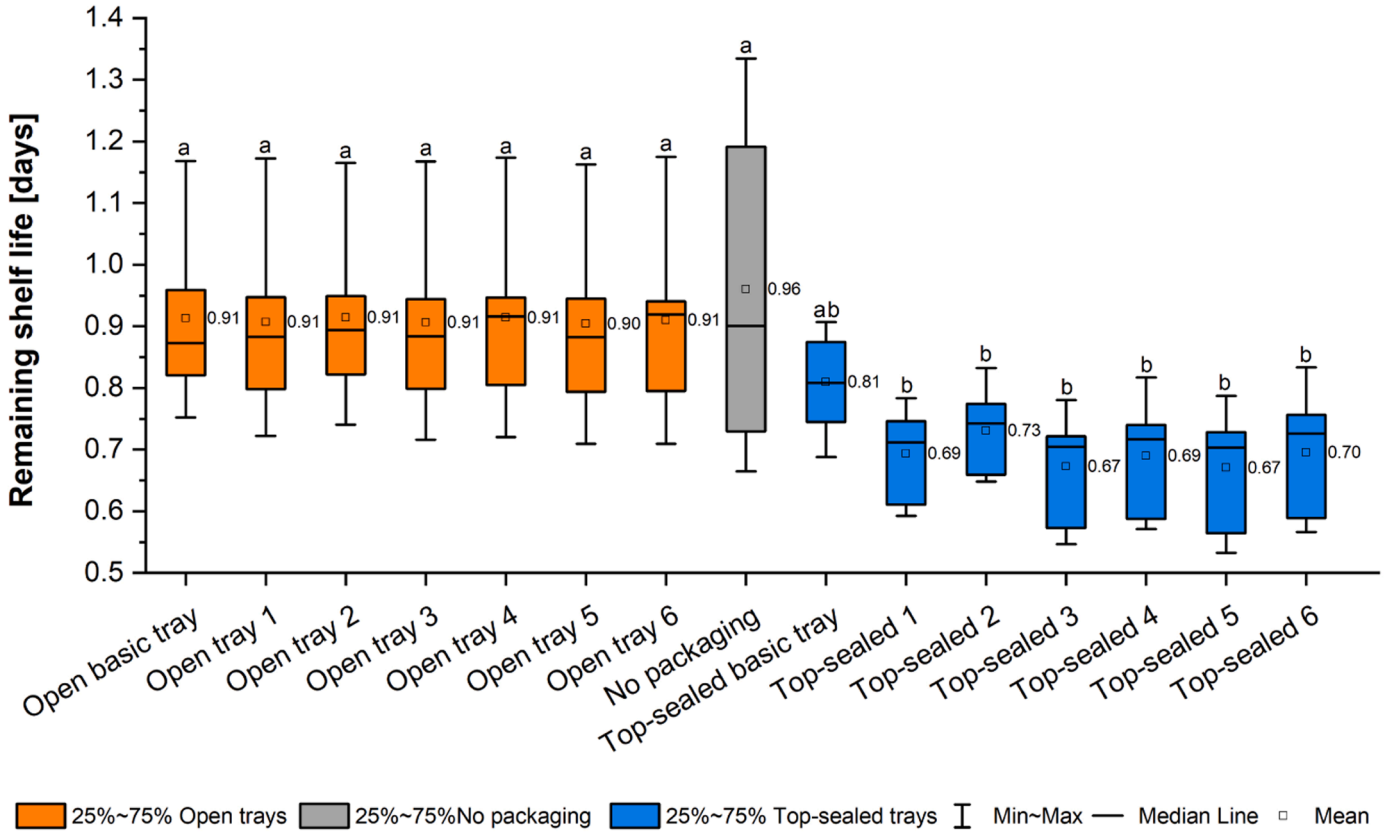

Fig. 14. Remaining respiration-driven shelf life [days] of strawberries in different trays after the 2.6 d simulated supply chain. Each boxplot represents one tray with 16 berries in it. The numbers next to the box show the mean value. Values with the same letter are not significantly different, $p<0.05$.

Longer TOW but less mass loss. We suggest that the optimal package would be in the middle of this trade-off. Nevertheless, in this study, no significant differences in TOW were found in the ventilated trays. Furthermore, the respiration-driven remaining shelf life needs to be considered to seek out the best package. The packages with the longest remaining shelf life on average are colored in blue, which are all the open-trays as well as the no packaging scenario. As expected, they are located in the middle of the diagram and, therefore, in the middle of the trade-off between condensation and mass loss.

The observations in sections 3.24–3.26 showed that the airflow inside the trays affects not only condensation but also mass loss and is, therefore, a key parameter influencing this trade-off. High flow rates minimize condensation but promote mass loss.

3.4. Which packaging design performs best along the supply chain, and what is the optimal TOA?

Because various trade-offs arise in designing the optimal package and many extrinsic aspects play an important role, there is not only one single package that is the best for every strawberry supply chain. However, choosing the packaging that balances out the three main analyzed quality metrics – condensation, mass loss, and respiration-driven shelf life – the best is a promising strategy to preserve the berries along their post-harvest journey. Every supply chain is individual in terms of hygrothermal conditions, length, number of stakeholders, etc. Therefore, we suggest selecting the packaging according to the specific supply chain.

In this specific case, where we assumed a 2.6 d long trip of the berries from Spain to Switzerland via several stakeholders, the best-performing packaging, by balancing out the trade-offs, are open trays 4 and 6, as shown in Fig. 15. Interestingly, open tray 4, which has a TOA of 5.6%, performs better than open tray 5, which has a TOA of 7.2%. We conclude that the arrangement of the vents has a substantial positive influence on the quality of the strawberries. Therefore, there is a limited additional value of a TOA $> 5.6\%$.

Another advantage of open trays is that no plastic is used since the trays can be made out of cardboard. Nevertheless, large retail stores often prefer not to use open trays. The reason for that is that people pick berries out of the trays, particularly if they are sold as units. Furthermore, it is less hygienic. For import supply chains, open trays are also less frequently used due to the risk of additional mass loss. In a longer supply chain, top-sealed trays might be the better choice as well because of the additional protection and the lower risk of condensation, which is actually the biggest hurdle in the market.

There are many more factors, such as variety of the berries, weather during harvest, ripeness of the berries, or season, that influence the quality as well. However, effective cooling and proper transportation are important in any case.

4. Conclusion and outlook

In this study, several ventilated packaging designs for fresh strawberries were investigated with the aim of finding an optimized packaging strategy in order to minimize the quality losses of strawberries along the whole supply chain. Therefore, models of twelve newly designed open- and top-sealed strawberry trays were created individually. With hygrothermal data from actual supply chains as input, these models mimicked how the berries physiologically and hygrothermally evolve inside the packaging along the supply chain. To compare the different packaging designs, actionable metrics like 7/8 cooling time, mass loss, time of wetness due to condensation, and respiration-driven remaining quality and shelf life were defined. Furthermore, the influence of the space between the top of the trays and the secondary packaging, as well as the aerodynamic performance, were studied. The designed new strawberry trays were compared to models of standard trays, which are being used in commercial supply chains and are much less ventilated. The key conclusions derived from this study are summarized below:

- Homogenous airflow inside the packaging is crucial for efficient cooling of the berries. Therefore, the vents should be placed in a way that the air can flow around the berries best possible during precooling but also during transport, in case the cargo was not fully precooled. Strawberries cool significantly faster in our newly-designed ventilated trays than in existing trays, and condensation-based time of wetness could be reduced by 45% due to ventilation in a top-sealed tray. Also, ventilation reduces the packaging's aerodynamic resistance. In addition, the height of the secondary packaging is an important measure, which does not only influence the aerodynamic performance, but also, the quality along the supply chain. More space above a single strawberry tray leads to a lower pressure loss but, in turn, to more condensation.
- Not only the total opening area [%] is an important packaging parameter, but also the size and the placement have a substantial influence on the performance of the packaging. We recommend a Total Open Area (TOA) between 5.5% and 7%. In this study, the diameter of the vents ranged between 5 and 12 mm. The vents should be evenly distributed, and ideally, berries should not block them. We designed an optimal packaging where vent hole blockage was minimized to promote ventilation.
- The variability in cooling performance and quality metrics within one tray is generally larger in open trays than in top-sealed trays. The largest differences are found in open trays between the berries on top and the berries in the middle on the bottom. The heterogeneity in ventilated top-sealed trays is smaller as a consequence of higher airspeeds that are reached inside the trays. Less air is bypassing the tray, and more is entering the packaging via the vent holes. Hence, the impact of additional ventilation is bigger in top-sealed trays than in open trays.
- There is always a trade-off in packaging design: A reduced risk of condensation comes along with a higher mass loss of the strawberries. Therefore, there is not one optimal packaging for all supply chains. Packaging should be chosen based on the specific needs of the intended supply chain.In this study, the best-performing trays, by balancing out the trade-offs, were two open trays with a TOA of 5.6% and 7.2%, respectively. Hence, if the vents are placed appropriately, a TOA of 5.6% is sufficient to preserve the strawberries better along the supply chain.

The models of the strawberry packaging enabled a unique insight into the quality evolution of the fruits along the supply chain and visualized the spatial distribution of condensation and mass loss. However, in reality, strawberries are transported on pallets in trailers, which have a large influence on the airflow and the hygrothermal conditions around the berries. In this study, only a single strawberry tray was analyzed. Therefore, future studies could assess the evolution of the strawberries along the supply chain, taking into account several trays, pallets and even the whole trailers. There are plenty of possibilities to further extend the model to better understand where and why quality losses occur and to minimize them. Also, mechanical stability of trays or energy consumption could be implemented. However, the single tray model is a valuable basis and helps to understand and build larger models.

In addition to that, with real-time wireless data retrieved from sensors, such models would be a promising tool for decision-making to all stakeholders along the supply chain of horticultural products. This means that the product quality of a current shipment can be monitored in real-time and even be predicted (Defraeye et al., 2021). Hence, the cargo can be handled accordingly, logistics could be improved, and food loss prevented and minimized.

Besides selecting the most suitable package, various actions along the supply chain could be taken to better preserve these delicate fruits.

The hygrothermal conditions at the retail stores, for example, are far from optimal and negatively affect the shelf life. Keeping the temperatures low and the relative humidity higher would prolong the shelf life of the berries. This could be done by displaying them in refrigerated displays or using dry misting to cool the air around the berries and increase the relative humidity. However, the efficiency of these techniques is again dependent on the packaging design (Shrivastava et al., 2023).

Declaration of Generative AI and AI-assisted technologies in the writing processs

During the preparation of this work, the authors used Grammarly (full paper) in order to improve the spelling, grammar, and style of the text. No additional original content was generated using these AI-assisted technologies. After using this tool/service, the authors reviewed and edited the content as needed and took full responsibility for the content of the publication.

CRediT authorship contribution statement

Elisabeth Annia Tobler: Writing – review & editing, Writing – original draft, Visualization, Methodology, Data curation, Conceptualization. **Fátima Pereira da Silva:** Writing – review & editing. **Chandrima Shrivastava:** Writing – review & editing, Methodology. **Deniz Turan:** Writing – review & editing. **Thijs Defraeye:** Supervision, Project administration, Funding acquisition, Conceptualization. **Celine Verreydt:** Writing – review & editing. **Leo Lukasse:** Writing – review & editing.

Declaration of Competing Interest

The authors declare that they have no known competing financial interests or personal relationships that could have appeared to influence the work reported in this paper.

Data availability

Data will be made available on request.

Acknowledgements

This work was financially supported by Sensitech, Coop Genossenschaft and Driscoll's, and subsidized by the Dutch Ministry of Economic Affairs and Climate Policy (EZK) through TKI Dinalog and the Topsector Logistics. The funders were not involved in the study design, collection, analysis, interpretation of data, the writing of this article, or the decision to submit it for publication. This manuscript has been released as a pre-print.

References

ASHRAE. (2010). Thermal Properties of Food. In 2010: *ASHRAE Handbook: Refrigeration.*

Bastarrachea, L., Dhawan, S., Sablani, S.S., 2011. Engineering properties of polymeric-based antimicrobial films for food packaging. Food Eng. Rev. *3* (2), 79–93. https://doi.org/10.1007/s12393-011-9034-8.

Becker, B.R., Misra, A., Fricke, B.A., 1996. Bulk refrigeration of fruits and vegetables part I: theoretical considerations of heat and mass transfer. HVAC R. Res. *2* (2), 122–134. https://doi.org/10.1080/10789669.1996.10391338.

Berry, T.M., Fadiji, T.S., Defraeye, T., Opara, U.L., 2017. The role of horticultural carton vent hole design on cooling efficiency and compression strength: a multi-parameter approach. Postharvest Biol. Technol. *124*, 62–74. https://doi.org/10.1016/j.postharvbio.2016.10.005.

Cagnon, T., Méry, A., Chalier, P., Guillaume, C., Gontard, N., 2013. Fresh food packaging design: a requirement driven approach applied to strawberries and agro-based materials. Innov. Food Sci. Emerg. Technol. *20*, 288–298. https://doi.org/10.1016/J.IFSET.2013.05.009.

Castelló, M.L., Fito, P.J., Chiralt, A., 2010. Changes in respiration rate and physical properties of strawberries due to osmotic dehydration and storage. J. Food Eng. *97* (1), 64–71. https://doi.org/10.1016/J.JFOODENG.2009.09.016.

Colussi, R., Ferreira da Silva, W.M., Biduski, B., Mello El Halal, S.L., da Rosa Zavareze, E., Guerra Dias, A.R., 2021. Postharvest quality and antioxidant activity extension of strawberry fruit using allyl isothiocyanate encapsulated by electrospun zein ultrafine fibers. Lwt *143* (December 2020)), 111087. https://doi.org/10.1016/j.lwt.2021.111087.

Concha-Meyer, A., Eifert, J., Wang, H., Sanglay, G., 2018. Volume estimation of strawberries, mushrooms, and tomatoes with a machine vision system. Int. J. Food Prop. *21* (1), 1867–1874. https://doi.org/10.1080/10942912.2018.1508156.

Corradini, M.G., 2018. Shelf life of food products: from open labeling to real-time measurements. Annu. Rev. Food Sci. Technol. *9*, 251–269. https://doi.org/10.1146/annurev-food-030117-012433.

De Castro, Larissa R., Vigneault, Clément, Cortez, L.A.B., 2004. Container opening design for horticultural produce cooling efficiency Retirement View project Studies on Sustainable Bioenergy View project Clément Vigneault Ingenierie Postrecolte / Postharvest Engineering. Food Agric. Environ. ⟨https://www.researchgate.net/publication/266034015⟩.

Defraeye, T., Cronjé, P., Berry, T., Opara, U.L., East, A., Hertog, M., Verboven, P., Nicolai, B., 2015. Towards integrated performance evaluation of future packaging for fresh produce in the cold chain (Elsevier Ltd). Trends Food Sci. Technol. Vol. 44 (Issue 2), 201–225. https://doi.org/10.1016/j.tifs.2015.04.008.

Defraeye, T., Lambrecht, R., Delele, M.A., Tsige, A.A., Opara, U.L., Cronjé, P., Verboven, P., Nicolai, B., 2014. Forced-convective cooling of citrus fruit: cooling conditions and energy consumption in relation to package design. J. Food Eng. *121* (1), 118–127. https://doi.org/10.1016/j.jfoodeng.2013.08.021.

Defraeye, T., Shrivastava, C., Berry, T., Verboven, P., Onwude, D., Schudel, S., Bühlmann, A., Cronje, P., Rossi, R.M., 2021. Digital twins are coming: will we need them in supply chains of fresh horticultural produce? Trends Food Sci. Technol. *109*, 245–258. https://doi.org/10.1016/J.TIFS.2021.01.025.

Delele, M.A., Ngcobo, M.E.K., Getahun, S.T., Chen, L., Mellmann, J., Opara, U.L., 2013. Studying airflow and heat transfer characteristics of a horticultural produce packaging system using a 3-D CFD model. Part II: Effect of package design. Postharvest Biol. Technol. *86*, 546–555. https://doi.org/10.1016/J.POSTHARVBIO.2013.08.015.

Elansari, A.M., Mostafa, Y.S., 2020. Vertical forced air pre-cooling of orange fruits on bin: Effect of fruit size, air direction, and air velocity. J. Saudi Soc. Agric. Sci. *19* (1), 92–98. https://doi.org/10.1016/j.jssas.2018.06.006.

Getahun, S., Ambaw, A., Delele, M., Meyer, C.J., Opara, U.L., 2017. Analysis of airflow and heat transfer inside fruit packed refrigerated shipping container: Part II – Evaluation of apple packaging design and vertical flow resistance. J. Food Eng. *203*, 83–94. https://doi.org/10.1016/j.jfoodeng.2017.02.011.

Kelly, K., Madden, R., Emond, J.P., do Nascimento Nunes, M.C., 2019. A novel approach to determine the impact level of each step along the supply chain on strawberry quality. Postharvest Biol. Technol. *147*, 78–88. https://doi.org/10.1016/J.POSTHARVBIO.2018.09.012.

Ktenioudaki, A., O'Donnell, C.P., do Nascimento Nunes, M.C., 2019. Modelling the biochemical and sensory changes of strawberries during storage under diverse relative humidity conditions. Postharvest Biol. Technol. *154*, 148–158. https://doi.org/10.1016/J.POSTHARVBIO.2019.04.023.

Liberty, J.T., Ugwuishiwu, B.O., Pukuma, S.A., Odo, C.E., 2013. Principles and application of evaporative cooling systems for fruits and vegetables preservation. Int. J. Curr. Eng. Technol. *3* (3), 1000–1006.

Linke, M., Geyer, M., 2013. Condensation dynamics in plastic film packaging of fruit and vegetables. J. Food Eng. *116* (1), 144–154. https://doi.org/10.1016/j.jfoodeng.2012.11.026.

Linke, M., Praeger, U., Mahajan, P.V., Geyer, M., 2021. Water vapour condensation on the surface of bulky fruit: some basics and a simple measurement method. J. Food Eng. *307*, 110661 https://doi.org/10.1016/J.JFOODENG.2021.110661.

Lufu, R., Ambaw, A., Opara, U.L., 2020. Water loss of fresh fruit: influencing pre-harvest, harvest and postharvest factors. Sci. Hortic. *272* (June) https://doi.org/10.1016/j.scienta.2020.109519.

Lufu, R., Ambaw, A., Berry, T.M., Opara, U.L., 2020. Evaluation of the airflow characteristics, cooling kinetics and quality keeping performances of various internal plastic liners in pomegranate fruit packaging. Food Packag. Shelf Life *26* (May)), 100585. https://doi.org/10.1016/j.fpsl.2020.100585.

Mercier, S., Brecht, J.K., Uysal, I., 2019. Commercial forced-air precooling of strawberries: a temperature distribution and correlation study. J. Food Eng. *242* (June 2017), 47–54. https://doi.org/10.1016/j.jfoodeng.2018.07.028.

Mukama, M., Ambaw, A., Opara, U.L., 2020. Advances in design and performance evaluation of fresh fruit ventilated distribution packaging: a review (Elsevier Ltd). Food Packag. Shelf Life Vol. 24. https://doi.org/10.1016/j.fpsl.2020.100472.

Ngo, I.L., Jeon, S., Byon, C., 2016. Thermal conductivity of transparent and flexible polymers containing fillers: a literature review. Int. J. Heat. Mass Transf. *98*, 219–226. https://doi.org/10.1016/j.ijheatmasstransfer.2016.02.082.

Pathare, P.B., Opara, U.L., Vigneault, C., Delele, M.A., Al-Said, F.A.J., 2012. Design of packaging vents for cooling fresh horticultural produce. Food Bioprocess Technol. Vol. 5 (Issue 6), 2031–2045. https://doi.org/10.1007/s11947-012-0883-9.

Poós, T., Varju, E., 2020. Mass transfer coefficient for water evaporation by theoretical and empirical correlations. Int. J. Heat. Mass Transf. *153*, 119500 https://doi.org/10.1016/j.ijheatmasstransfer.2020.119500.

Robinson, J.E., M, B.K., Burton, W.G., 1975. Storage characteristics of some vegetables and soft fruits. Ann. Appl. Biol. *81* (3), 399–408. https://doi.org/10.1111/j.1744-7348.1975.tb01656.x.

Schudel, S., Shrivastava, C., Rebeaud, S.G., Karafka, L., Shoji, K., Onwude, D., Defraeye, T., 2022. Combining experiments and mechanistic modeling to compare ventilated packaging types for strawberries from farm to retailer. SSRN Electron. J. 1–16. https://doi.org/10.2139/ssrn.4103973.

Shoji, K., Schudel, S., Onwude, D., Shrivastava, C., Defraeye, T., 2022. Mapping the postharvest life of imported fruits from packhouse to retail stores using physics-based digital twins. Resour. Conserv. Recycl. *176*, 105914 https://doi.org/10.1016/J.RESCONREC.2021.105914.

Shrivastava, C., Schudel, S., Shoji, K., Onwude, D., da Silva, F.P., Turan, D., Paillart, M., Defraeye, T., 2023. Digital twins for selecting the optimal ventilated strawberry packaging based on the unique hygrothermal conditions of a shipment from farm to retailer. Postharvest Biol. Technol. *199*, 112283 https://doi.org/10.1016/J.POSTHARVBIO.2023.112283.

Sousa-Gallagher, M.J., Mahajan, P.V., Mezdad, T., 2013. Engineering packaging design accounting for transpiration rate: model development and validation with strawberries. J. Food Eng. *119* (2), 370–376. https://doi.org/10.1016/j.jfoodeng.2013.05.041.

Tano, K., Kamenan, A., Arul, J., 2009. Respiration and transpiration characteristics of selected fresh fruits and vegetables. Agron. Afr. *17* (2) https://doi.org/10.4314/aga.v17i2.1662.

Trinetta, V., McDaniel, A., Batziakas, K.G., Yucel, U., Nwadike, L., Pliakoni, E., 2020. Antifungal packaging film to maintain quality and control postharvest diseases in strawberries. Antibiotics *9* (9), 1–12. https://doi.org/10.3390/antibiotics9090618.

Wang, J., Gardner, D.J., Stark, N.M., Bousfield, D.W., Tajvidi, M., Cai, Z., 2018. Moisture and oxygen barrier properties of cellulose nanomaterial-based films. ACS Sustain. Chem. Eng. *6* (1), 49–70. https://doi.org/10.1021/acssuschemeng.7b03523.

Wang, D., Lai, Y., Zhao, H., Jia, B., Wang, Q., Yang, X., 2019. Numerical and experimental investigation on forced-air cooling of commercial packaged strawberries. Int. J. Food Eng. *15* (7) https://doi.org/10.1515/ijfe-2018-0384.

Wu, W., Cronjé, P., Verboven, P., Defraeye, T., 2019. Unveiling how ventilated packaging design and cold chain scenarios affect the cooling kinetics and fruit quality for each single citrus fruit in an entire pallet. Food Packag. Shelf Life *21*. https://doi.org/10.1016/j.fpsl.2019.100369.

Zou, Q., Opara, L.U., McKibbin, R., 2006. A CFD modeling system for airflow and heat transfer in ventilated packaging for fresh foods: I. Initial analysis and development of mathematical models. J. Food Eng. *77* (4), 1037–1047. https://doi.org/10.1016/J.JFOODENG.2005.08.042.